DEMOGRAPHICS, TRADE, AND GROWTH *

YANG PEI †

MAY 11, 2025

CLICK HERE TO GET THE MOST UPDATED VERSION

ABSTRACT

Motivated by China's recent economic slowdown, the relocation of labor-intensive industries, and an aging population, this paper examines how demographic forces shape China's economic growth and trade patterns. Country-level panel regressions indicate that countries with a larger working-age population share experience higher productivity growth and investment share of GDP. Building on these findings, I develop and calibrate an overlapping generations (OLG) trade model with three key features: age-varying abilities to generate ideas that drive knowledge accumulation, age-varying saving behaviors affecting capital accumulation, and a multi-sector structure that integrates both Heckscher-Ohlin and Ricardian comparative advantage forces. Through comparing the baseline case to a hypothetical case where China's fertility and/or survival rates align with those of the rest of the world, I find a trade-off in China's demographics: a savings-favorable age distribution in the short term leads to gains in capital and income per worker, along with a stronger comparative advantage in capital-intensive sectors. However, in the long term, it results in a lower growth path for productivity and income per worker, as a smaller working-age population generates fewer new ideas after 2060.

Keywords: Demographics; Idea generation; Capital accumulation; International trade; Comparative advantage; Trade patterns change; Economic growth

JEL Codes: E21, F11, J11, O47, O11.

*I am deeply indebted to Kei-Mu Yi for his invaluable guidance. I also extend my sincere appreciation to my committee members, German Cubas, Bent Sorensen for their endless help. I am particularly grateful to Manuel Amador, George Alessandria, Max Dvorkin, Radek Paluszynski, Michael Sposi, Michael Waugh and all participants in various seminars and conferences for their encouragements and insightful comments. All errors are my own.

†Department of Economics, University of Houston E-mail: ypei5@uh.edu.

1. Introduction

In recent decades, the world has faced significant demographic shifts, notably characterized by population aging and decline. By 2021, approximately 31% of global GDP was generated in countries experiencing population decline, many of which are also grappling with more pronounced decline in working-age population. Among these countries, China, as the world's second-largest economy, stands out as one of the most important. As its population declines and ages, its economic growth is also slowing down.

China's growth over the past several decades has mainly relied on a robust labor supply and substantial productivity improvements. On the one hand, by opening up to trade, China leveraged its comparative advantage in labor-intensive goods, benefiting from specialization and trade. On the other hand, productivity growth during this period per se also contributed to the economic growth. However, the forces that fueled China's past growth are now shifting. The nation faces an aging and shrinking population alongside a slowdown in productivity growth. These demographic changes, along with rising wages, will gradually erode China's comparative advantage in labor-intensive production. Additionally, a lower working-age share will dampen savings and hinder capital accumulation, further complicating the transition to capital-intensive goods.

This transformation raises a critical question: how have demographic changes influenced China's trade patterns and economic growth in the past, and how will these forces continue to shape its future performance? As we know from economic theory, productivity and capital are widely recognized as drivers of economic growth. Furthermore, differences in productivity and capital-labor endowments are key to explaining shifts in trade patterns. Therefore, I aim to answer this question centered around two mechanisms, age-dependent saving behavior and age-dependent ideas generation process, utilizing both empirical analysis and theoretical modeling.

In the empirical part, I examine the relation between demographic structure and productivity, as well as other macroeconomic variables. I finds that countries with a higher proportion of working-age people tend to exhibit higher TFP growth rates and greater shares of investment in GDP.[1]

In the theoretical part, I develop an overlapping generations (OLG) open-economy model that incorporates three key features. First, age-varying abilities to generate ideas influence changes in productivity. Second, age-dependent saving behavior affects capital accumula-

1. In fact, at the micro level, existing literature shows that individuals in middle age tend to be more productive and creative than their younger and older counterparts. These facts contribute to the micro-level mechanism underlying the observed positive link at the macro (country) level (Feyrer, 2008; Werding, 2008; Sevilla et al., 2007; Werding et al., 2007; Kögel, 2005).

tion. Third, by incorporating multiple sectors and including both capital and labor in the production function, the model captures the forces of both Heckscher-Ohlin and Ricardian comparative advantage.

I use this model to explain how demographic changes have shaped trade patterns and economic growth in the past, and to project future developments based on these dynamics. Through comparing the baseline case to a hypothetical case where China's fertility and/or survival rates align with those of the rest of the world, I find a trade-off in China's demographics: a savings-favorable age distribution in the short term leads to gains in capital and income per worker, along with a stronger comparative advantage in capital-intensive sectors. However, in the long term, it results in a lower growth path for productivity and income per worker, as a smaller working-age population generates fewer new ideas after 2060.

In the model, the main driving forces—age-time varying fertility rates and survival rates—mediated through the model's mechanisms, affect both sectoral productivities and capital accumulations. These forces, together with the exogenous trade cost changes, affect the sectoral prices, which, in turn, affects the allocation of production across sectors and locations, and ultimately affects both trade patterns and economic performance. For example, a higher survival rate leads to greater knowledge stock and capital stock accumulation, raising the balanced growth path by enhancing both productivity and capital. Free trade induce specialization, which encourages higher productivity and lowers prices, ultimately leading to even greater capital accumulation. In addition, A lower fertility rate impacts both knowledge and capital stocks. In the short run, a reduced young population raises capital per person, temporarily boosting economic output. However, over time, this benefit is offset by slower productivity growth due to the demographic shift, ultimately causing capital per person to fall below the previous growth path. Trade liberalization can mitigate this long-term drawback by maintaining capital per person above the old growth path for a longer period, which extends the overall economic benefits in comparison to a closed economy scenario.

I calibrate the model with five country groups and five sectors, covering the period from 1970 to 2100. For forward-looking households, it is essential to define the time-varying processes that extend beyond the sample period of 1970–2020. The additional 80 years (2020–2100) are deliberately designed to establish robust expectations for individuals born in 2020, the final year of interest. Consequently, the model is calibrated and solved from the assumed initial steady state in 1970 to the final steady state in 2100. Historical data are used for calibration from 1970–2020, while data or shocks for the period from 2021–2200 are based on projections and imputations. Specifically, I imputed value-added shares and sectoral intermediate input shares in production, as well as sectoral shares in aggregate investments and consumption, using input-output tables. Fertility rates and survival rates are derived from the UN demographic database. The main time-varying variables—sectoral fundamental productivities and trade costs—are calibrated using data on trade flows, input-output tables, capital stock, demographic variables, and sectoral prices.

The calibration results show that, compared to other economies, China's fertility rate experienced a more rapid first-round decline between 1970 and 1980, followed by a second-round decline from 1990 to 2000. The unconditional survival rate at age 65 generally follows a similar upward trend as other economies but remains lower than that of advanced economies throughout the entire period, while being higher than that of the Rest of the World (RoW). China's productivity exhibits an upward trend across all sectors, growing at a faster pace than in other regions despite starting from a lower initial level. Overall, trade costs are higher in the services sector, but trade barriers decline across all sectors, with a faster rate of decline in the manufacturing sectors. Finally, I feed the calibrated parameters and shocks back into the model, and the generated results align well with real data, including sectoral trade flows, total sectoral output, value-added, capital stock, wage rates, rental rates, and sectoral prices.

To assess the role of each driving force affecting economic growth and trade patterns over time, I conduct three counterfactual exercises. First, I remove both the demographic-induced-saving effects and demographic-induced-productivity changes. Specifically, I replace the age-varying fertility and survival rates in China with those of the rest of the world (RoW) and allow productivity to change in response to changes in demographics. I refer to this as the *without demographic scenario*. Second, I remove only the demographic-induced-saving effects. In this scenario, I again replace China's age-varying fertility and survival rates with those of the RoW but retain the usual productivity changes. I call this the *demographic-capital channel scenario*. Third, I remove only the demographic-induced-productivity effects. In this case, I maintain the original age-varying fertility and survival rates of China and its implied demographic process. However, I allow productivity to change as if China's demographic structure were aligned with that of the rest of the world (RoW), where China's age-varying fertility and survival rates mirror those of the RoW. I refer to this as the *demographic-idea channel scenario*. For each counterfactual scenario, I calculate the dynamic equilibrium as it transitions from one balanced growth equilibrium to another, guided by the corresponding exogenous processes under perfect foresight. All three scenarios start from the same initial equilibrium but converge to different final equilibria, each determined by the projected demographic processes at the final year.

Counterfactual analysis reveals that China's demographic characteristics, a lower fertility rate and higher survival rate relative to the rest of the world (RoW), generate a short-run and long-run trade-off for real income per worker. In the short run, the *demographic-capital channel* exerts a stronger influence than the *demographic-idea channel*. Under a lower fertility rate and higher survival rate compared to the RoW, China's demographic structure in the short run is characterized by a higher share of working-age and senior working-age populations. Consequently, this age structure, which is more conducive to savings, through the *demographic-capital channel*, increases the level of capital stock per worker, leading to higher real income per worker. In parallel, this structure also enhances China's comparative advantage in capital-intensive sectors compared to the counterfactual scenario. Specifically, compared to the counterfactual scenario in which China's fertility rate and survival rate are replaced by those of the RoW, by 2020, China's real income per worker is approximately 5.08% higher, and China's revealed comparative advantage index in capital-intensive sectors is around 6.79% higher than the counterfactual level. These short-run trends are projected to persist until 2060.

In the long run, however, the *demographic-idea channel* becomes more influential than the *demographic-capital channel*. After 2060, China's demographic process (characterized by a lower fertility rate and higher survival rate compared to the RoW) implies a reduced number of working-age population. Fewer workers suggest fewer new ideas, which in turn lower the productivity growth path. Consequently, the *demographic-idea channel* leads to a lower level of real income per worker than the counterfactual scenario. By 2070, compared with the counterfactual in which China's fertility rate and survival rate are substituted with those of the RoW, China's projected real income per worker is estimated to be approximately 4.08% less than the counterfactual level.

Related Literature This paper contributes to three strands of literature. First, it connects to the literature on demographic structure and productivity, both empirically and theoretically. On the empirical side, several studies have examined the relationship between age structure and productivity at both the macro and micro levels. At the macro level, studies have shown that the age composition of populations has significant effects on a country's productivity Feyrer (2007); Maestas, Mullen, and Powell (2023). At the micro level, based on data from patents and innovation, Jones (2010) have shown that people's ability to generate ideas varies with age. These findings indicate that shifts in the age composition within a country may influence productivity through the quality of innovation and the generation of new ideas. In my paper, due to data availability, I replicate these results at the macro level, using more countries and more recent years.

On the theoretical side, this paper relates to literature exploring the mechanisms through which demographic changes influence productivity from three perspectives. First, some models incorporate age-dependent productivity, where the effectiveness of labor varies by age cohort, as seen in the work of Lindh and Malmberg (1999). Second, models of endogenous growth, such as those by Becker, Murphy, and Tamura (1990), show that demographic changes can alter incentives for investment in human capital, which in turn affects productivity growth. Third, recent work by Aksoy, Basso, Smith, and Grasl (2019) develops a framework where age structure affects a country's innovation rate by influencing the distribution of skills and experience across the population. In this paper, I model the demographic-productivity relationship through the assumption of age-varying ability in generating new ideas. Specifically, Buera and Oberfield (2020) builds the dynamics of knowledge stock through the process of exogenous idea arrival and learning from the external ideas distribution. I further assume that people of varying ages differ in their ability to find new ideas, and I introduce more sectors.

Second, this paper relates to the literature on multi-country trade models with capital accumulation. Among the most relevant is Sposi (2022), which examines how demographic transitions impact global trade imbalances through a multi-country Ricardian trade model. Other papers in this field include Eaton, Kortum, Neiman, and Romalis (2016), Alvarez (2017), Ravikumar, Santacreu, and Sposi (2019), Anderson, Larch, and Yotov (2020), and Sposi, Yi, and Zhang (2021a), with specific focuses other than demographics. However, my paper differs by linking capital accumulation with demographics varying by ages, offering a novel perspective on the interplay between demographics, trade-induced relocation, and economic growth.

Third, this paper is related to two strands of literature on trade and the Chinese economy. The first strand involves research on explaining and quantifying the forces driving China's growth through a trade perspective, either at the aggregate or distributional level. This research often incorporates internal migration and internal trade across China's regions into trade models, emphasizing the effects of internal migration or internal trade to varying degrees, depending on the paper's focus, such as in Liu and Ma (2018); Tombe and Zhu (2019); Fan (2019); Hao, Sun, Tombe, and Zhu (2020); Ma and Tang (2020). In addition, there is a wealth of research focused on explaining changes in China's trade patterns per se. This strand is represented by papers such as those by Alessandria, Khan, Khederlarian, Ruhl, and Steinberg (2021); Hanwei, Jiandong, and Yue (2024). My paper focuses on quantifying both trade pattern changes and economic growth from a demographic perspective, which has yet to be explored in previous papers.

The rest of the paper is organized as follows. Section 2 provides the empirical analysis. Section 3 describes the model and demonstrate how the model works. Section 4 describes the data, calibrates the main parameters and shocks, and then briefly discusses the calibrated shocks and model fitness. Section 5 conduct counterfactual analysis, and Section 6 concludes.

2. Empirical Evidence

The empirical analysis incorporated three types of variables. Firstly, there were 7 types of demographic structure indices, including the dependency ratio, young dependency ratio, old dependency ratio, working age share, young population share, old population share, and population distribution across different age cohorts. These variables were calculated or directly obtained from the United Nations World Population Prospects report. Secondly, the total factor productivity (TFP) growth was calculated based on TFP data from the Penn World Table 10.01. Thirdly, various other macroeconomic outcomes, including investment, consumption share of GDP, and real GDP per capita, were acquired from the World Development Indicators database.

Regression model 1

The relationship between demographic variables and technology change is examined by estimating the following model:

$$GRTFP_{it,t+4} = Constant + \beta_1 Demographic_{it} + \beta_2 Control_{it} + f_i + f_t + \varepsilon_{it} \ . \tag{1}$$

where i means country, t means year. The dependent variable $GRTFP_{it,t+4}$ means average TFP growth rate (%) for country i during the period from t to $t+4$, and calculated as follows:

$$GRTFP_{it,t+4} = \left(\frac{TFP_{i,s+4}}{TFP_{i,s}}\right)^{\frac{1}{4}} - 1$$

Regression model 2

Similarly, the relationship between demographic variables and macroeconomic outcomes (capital formation, and consumption) is examined by estimating the following model:

$$Ave.Y_{it,t+4} = Constant + \beta_1 Demographic_{it} + f_i + f_t + \varepsilon_{it} \ . \tag{2}$$

The variable $Ave.Y_{it,t+4}$ means average investment, or consumption share of GDP (%) during the period t to $t+4$:

$$Ave.Y_{it,t+4} = \sum_{s=t+0}^{t+4} \frac{Y_{i,s}}{5}$$

The variable $Demographic_{it}$ represents demographic-relevant variables for country i at time t, such as the young dependency ratio, which is defined as the ratio of people aged (0-14) to people aged 15-64. The old dependency ratio is defined as the ratio of people aged 65 and above to people aged 15-64. The working age share is defined as the share of people aged 15-64. The young share is defined as the share of people aged 0-14, and the old share is defined as the share of people aged 65 and above, or the population share at different age cohorts. The variable $Control_{it}$ represents a control variable for country i at time t, specifically the initial log real GDP per person. f_i and f_t are country and time fixed effects.

I use panel data encompassing 76 countries across different income levels, spanning the period from 1975 to 2019. The selection of country groups and time periods for analysis was based on data availability, resulting in 34 high-income countries, 21 upper middle-income countries, 16 lower middle-income countries, and 5 lower-income countries according to the United Nations classifications.

As is common in the literature, I reduce the influence of business cycle fluctuations by calculating 5-year growth rates and dividing the entire period of 1975–2019 into nine non-overlapping 5-year sub-periods period 1 (1975–1979), period 2 (1980–1984), ..., and period 9 (2015–2019). Since I treat all demographic variables measured at the start of the sample period, before the growth has occurred, the regression analysis carries a stronger sense of causality. Similarly, in the following other types of regression, the time lag between the independent variables and the dependent variable reduces the likelihood of endogeneity issues caused by reverse causality. For the purpose of conducting robust checks, I performed the same regression analysis for five non-overlapping 8-year periods: period 1 (1980-1987), period 2 (1988-1995), ... , and period 5 (2012-2019).

TABLE 1

THE EFFECT OF DEMOGRAPHIC STRUCTURE CHANGE

	Average value in the future 4 years					
VARIABLES	Δ TFP/TFP		Cap.F.(% GDP)		Cons.(% GDP)	
Work.Share (15-64)/ToT	11.43***		28.80**		-33.75**	
	(3.33)		(2.17)		(-2.00)	
Child.Share (0-14)/ToT		-13.98***		-24.76*		33.75*
		(-3.68)		(-1.74)		(1.99)
Old.Share (65+)/ToT		2.79		-65.97***		33.77
		(0.39)		(-2.65)		(0.90)
Initial.Log.Dependent	-3.09***	-3.46***				
	(-4.82)	(-4.77)				
Constant	20.96***	35.46***	4.09	34.10***	98.56***	64.81***
	(3.65)	(5.19)	(0.53)	(6.74)	(9.84)	(9.15)
Observations	732	732	724	724	725	725
R-squared	0.259	0.266	0.575	0.581	0.753	0.753
Time FE	YES	YES	YES	YES	YES	YES
Country FE	YES	YES	YES	YES	YES	YES

Notes: Robust t-statistics in parentheses. *** $p < 0.01$, ** $p < 0.05$, * $p < 0.1$. The variable $Work.Share$ represents the working age share, which is defined as the share of people aged 15-64. The variable $Child.Share$ represents the young population share, which is defined as the share of people aged 0-14, and the variable $Old.Share$ represents old population share, which is defined as the share of people aged 65 and above. In Table B.4 from the appendix, indices such as patent applications per 1000 people and industrial design applications per 1000 people are also used to represent TFP changes as robust checks. I also use different index to capture the changes of age structure to ensure robustness of empirical estimates. For details, please refer to Appendix B.

Table 1 report the main results of the regression analysis. It shows that increasing young people share or decreasing working age share related to TFP growth rate decline, while increasing elderly share has positive but no significant effects on TFP growth rate. This results is similar with Kögel (2005). Specifically, 1 percentage point (p.p) increase, or 1 s.d. increase, in the working age share is associated with a corresponding increase of 0.11 percentage points (p.p), or increase of 0.81 s.d., in the average TFP growth rate over the following 4-year period.

It also shows that countries with a larger proportion of working-age individuals , or a lower share of elder or young people, or a lower dependency ratio tend to exhibit higher shares of investment in GDP, along with a lower share of consumption in GDP. While the increasing share of elderly population (age 65 and above) does not appear to have a significant impact on consumption. Specifically, a 1 percentage point (p.p) increase, or 1 standard deviation (s.d.) increase, in the working age share leads to a corresponding increase of 0.29 percentage points (p.p), or an increase of 0.33 standard deviations (s.d.), in the average capital formation share of GDP over the next four years. Meanwhile, a 1 percentage point (p.p) increase, or 1 standard deviation (s.d.) increase, in the working age share is associated with a subsequent decrease of 0.34 percentage points (p.p), or an increase of 0.21 standard deviations (s.d.), in the average consumption share of GDP over the following four years.

Overall, I find that countries with a higher proportion of working-age people tend to exhibit higher TFP growth rates and greater shares of investment in GDP, while having a smaller consumption share. These findings highlight the importance of considering the age structure's impact on productivity change, consumption, and investment behaviors. In the next section, I then develop a life-cycle model of demographics and trade, aligned with the key results presented here.

3. Model: An open-economy OLG model with semi-endogenous growth

The model builds on Ravikumar, Santacreu and Sposi (2019) and Sposi, Yi, and Zhang (2021b), with three key extensions. First, I integrate age-productivity links into the model, following the approach of Lucas Jr (2009), Alvarez, Buera, Lucas, et al. (2013), Alvarez, Buera, Lucas, et al. (2008), Buera and Oberfield (2020), and Cai, Caliendo, Parro, and Xiang (2022). Age-varying abilities to generate ideas become key mechanisms behind the knowledge stock accumulation. Second, I incorporate overlapping generations (OLG) features similar to those in Sposi (2022), where age-varying saving behavior influences capital accumulation. Third, by considering multiple sectors and incorporating both capital and labor into the production function, the model implicitly captures the forces of both Heckscher-Ohlin and Ricardian comparative advantage.

3.1. Firms

The model consists of N countries, each with J sectors. These countries and sectors are interconnected through input-output linkages. Firms in country n and sector j produce a continuum of goods. Every variety within each sector is tradable and indexed by $\omega \in [0,1]$, using a constant returns to scale (CRS) technology:

$$y_{n,t}^{j}(\omega) \equiv q_{n,t}^{j}(\omega)\left[L_{n,t}^{j}(\omega)^{\beta_n^j} K_{n,t}^{j}(\omega)^{1-\beta_n^j}\right]^{\gamma_n^j} \prod_{k=1}^{J} m_{n,t}^{k,j}(\omega)^{\gamma_n^{k,j}} \tag{3}$$

Here, $m_{n,t}^{k,j}(\omega)$ represents the quantity of intermediate composite goods from sector k used as inputs to produce $y_{n,t}^{j}(\omega)$ units of sector j variety ω, while $K_{n,t}^{j}$ and $L_{n,t}^{j}$ denote the quantities of capital and efficient labor used, respectively. The productivity of variety ω in country n and sector j, denoted $q_{n,t}^{j}(\omega)$, is a random variable that follows a Fréchet distribution: $F_{n,t}^{j}(q) = \exp\left(-\lambda_{n,t}^{j} q^{-\theta}\right)$. The mean of this distribution, $\lambda_{n,t}^{j}$, is commonly referred to as the knowledge stock.

The non-tradable sectoral composite intermediate good $Q_{n,t}^{j}$ in country n sector j is consistent with tradable intermediate good $q_{n,t}^{j}(\omega)$:

$$Q_{n,t}^{j} \equiv \left[\int_0^1 y_{n,t}^{j}(\omega)^{\frac{\sigma-1}{\sigma}} dj\right]^{\frac{\sigma}{\sigma-1}}. \tag{4}$$

The sectoral composite good $Q_{n,t}^{j}$ is used for final consumption ($C_{n,t}$), investment ($I_{n,t}$), and as an intermediate input in sector-k production: $\displaystyle\int_0^1 m_{n,t}^{j,k}(\omega), d\omega$.

3.1.1. Stock of knowledge

For the remaining paragraphs of this section, sector subscript j is omitted for simplicity.

For each economy n in which there is a continuum of intermediate varieties produced in the unit interval. For each variety, there is a large set of potential producers who have different technologies to produce the good. Each potential producer is characterized by the productivity of her idea, which we denote by q, to produce an intermediate variety.

Individuals of varying ages exhibit differences in their ability to generate new ideas. Between time t and time $t+1$, individuals of diverse ages within the economy can generate their new ideas to produce a variety, and producers are exposed to these new ideas to produce a variety. Both the number of new ideas and the productivity of them are stochastic, which generates randomness in the usage of the new ideas. The producer only adopts a new idea if the new ideas' productivity is greater than q. Specifically, Similar to Cai, Caliendo, Parro and Xiang (2022), the number of new ideas per unit of time to which the producer is exposed follows a Poisson distribution. For each external new idea that arrives to the producer corresponds to a new productivity for producing a variety, given by

$$q = zq\prime^{\rho}.$$

Producers combine random "original components", z, with random "external insights" or "external idea", q', to generate new productivity. The "original component" originates from their internal source of ideas, drawn from their own distribution of original ideas $H(z)$. The "external insights" are insights obtained from the arrived new idea, drawn from the current productivity distribution $F_t(q')$. ρ measures the diffuse rate of new ideas, also known as learning intensity. The current productivity distribution describes the set of insights that producers might access.

Between time t and time $t+1$, individual varies at ages generate new ideas and local producers are exposed to these new ideas about producing the variety. Among the arrived new ideas during t and $t+1$, the probability that the best new idea has productivity no greater than q for each age g producer is defined as $F_{t,g}^{best\ new}$. Under Assumption 1, one can derive Proposition 1, which characterizes the cumulative distribution function (C.D.F.) of the productivity of the best new idea.

Assumption 1

a) The number of new ideas arriving between t and $t+1$ follows a Poisson distribution with mean $\alpha_t \bar{z}^{-\theta}$. The term α_t controls the mean number of new ideas arriving between t and $t+1$.
b) Total mean number of new ideas arriaved between t and $t+1$ is defined as

$$\alpha_t \equiv \left[\sum_g \eta_g N_{n,g,t} \right]^{\varphi}$$

i) η_g controls the number of arrived new idea per unit of time per age g people

ii) $\varphi < 1$ reflects some kind of crowding effects, or duplication of idea. .

c) The Internal original idea z draw from Pareto distribution with C.D.F: $H(z) = 1 - (\frac{z}{\bar{z}})^{-\theta}$, where $\bar{z}$ is lower bound of support and shape parameter $\theta > 1$.
d) $\beta \in [0, 1)$ measures the strength of ideas diffusion .
e) F_t has sufficiently thin tail; i.e $\lim_{\bar{z} \to 0} \bar{z}^{-\theta} \left[1 - F_t \left(\left(\frac{q}{\bar{z}} \right)^{\frac{1}{\rho}} \right) \right] = 0$.

Under Assumption 1, between t and $t+1$, the C.D.F of the productivity of the best new idea is given by

$$F_t^{best\ new}(q) = exp \left(- \left(\sum_g \eta_g N_{n,g,t} \right)^{\varphi} q^{-\theta} \int_0^{\infty} x^{\rho\theta} dF_t(x) \right)$$

in the limiting case when $\bar{z} \to 0$.

The distribution of the productivity of best new idea during t and $t+1$ and local productivity distribution at t together determine the next period's local productivity distribution:

$$F_{t+1}(q) = F_t^{best\ new}(q)\, F_t(q)\,.$$

Assume that the initial frontier of knowledge at time t follows a Fréchet distribution given by $F_t(q) = exp(-\lambda_t q^{-\theta})$, one can get evolution of the stock of knowledge over time:

$$\lambda_{n,t+1} - \lambda_{n,t} = \left(\sum_g \eta_g N_{n,g,t}\right)^{\varphi} (\lambda_{n,t})^{\rho}\, \Gamma(1-\rho)\,. \tag{5}$$

Equation 5 implies that, on the one hand, a higher the number of arrived new idea per unit of time per age g people. (higher η_g) leads to a higher knowledge stock for the following period, which in turn implies a higher overall productivity level. On the other hand, at the steady state, λ_t grows at the constant rate g_λ, and $1 + g_\lambda = (1 + g_n)^{\varphi/(1-\rho)}$.

3.2. Households

In each region, households follow an overlapping generations framework. Households enter the economy at the age $g = 1$ and continues until either death or they reach the maximum age $g = G$. Households supply labor inelastically during their working years, specifically when g falls within the interval $[G_0 + 1, G_1]$, with $l_g = 1$. After retirement, which occurs when $g \in [G_1 + 1, G]$, their labor supply drops to $l_g = 0$. Let $N_{n,g,t}$ represent the number of households at age g that are alive at time t. We define $N_{n,t}$ as the total population in the economy at any given period t, which can be expressed as $N_{n,t} \equiv \sum_{g=1}^{G} N_{n,g,t}$.

The labor endowment for age group g, denoted $l_{n,g}$, is adjusted for average human capital (schooling), $E_{n,t}$.[2] Among the working-age population, a fraction $\tau_{n,t}^L$ are excluded from employment due to factors unrelated to age, such as business cycle conditions, female labor force participation rates, or distortions in the labor market. Hereafter, $\tau_{n,t}^L$ will be referred to as a labor market distortion. Let $L_{n,t}$ denote the total labor supply, and $L_{n,t}^e$ the total labor supply adjusted for average human capital. These can be defined as:

$$L_{n,t} = \left(1 - \tau_{n,t}^L\right) \sum_{g=G_0+1}^{G_1} N_{n,g,t} l_g; \quad L_{n,t}^e = E_{n,t} L_{n,t}. \tag{6}$$

To simplify the notation, I omitted country subscript n here. Population dynamics in the model are driven by exogenous fertility and survival rates. The variable $N_{g,t}$ represents the number of individuals aged g alive at time t. Fertility rates for households of age g at time t are denoted by $f_{g,t}$, while $s_{g,t}$ represents the survival probability from age $g-1$ to g.[3]

2. This adjustment means that the wage rate, $W_{n,t}$, reflects the price of an efficiency unit of labor.

3. Notably, $s_{G+1,t} = 0$, indicating that individuals live no longer than age G.

The demographic process follows:

$$N_{1,t+1} = s_{1,t} \sum_{g=1}^{G} f_{g,t} N_{g,t}; \quad N_{g+1,t+1} = s_{g+1,t+1} N_{g,t}.$$

3.2.1. Individual lifetime consumption and saving

For each country n, households of age g, born in period t, make decisions regarding their lifetime consumption $\{c_{n,g,t+g-1}\}_{g=1}^{G}$ and savings $\{b_{n,g+1,t+g}\}_{g=1}^{G-1}$ to maximize their expected lifetime utility, subject to the budget constraints and non-negativity constraints.

The lifetime utility for a cohort born in country n at time t is defined as:

$$\max_{\{c_{g,t+g-1}\}_{g=1}^{G}\{a_{g+1,t+g}\}_{g=1}^{G-1}} \sum_{g=1}^{G} \psi_{n,t+g-1} \beta^{g-1} S_{g,t+g-1} u(c_{g,t+g-1}); \text{ with } u(c_{g,t+g-1}) = \log(c_{g,t+g-1}).$$

The variable $\psi_{n,t}$ represents saving wedges, accounting for influences on saving that are not explained by demographic factors in the model. These influences include factors such as capital taxes and other country-specific distortions. The term $S_{g,t+g-1}$ denotes the unconditional probability that a household, born in period t, survives for g periods.

The budget and non-negativity constraints are given by:

$$\begin{aligned} P_{n,C,t+g-1} c_{n,g,t+g-1} + P_{n,I,t+g-1} a_{n,g+1,t+g} &= P_{n,I,t+g-1} \left(1 + r_{n,t+g-1}\right) a_{n,g,t+g-1} \\ + W_{n,t+g-1} \left(1 - \tau^{L}_{n,t+g-1}\right) E_{n,t+g-1} l_g + ts^{D}_{n,t+g-1} + ts^{T}_{n,t+g-1} & \quad \forall g \in [1, G] \end{aligned} \tag{7}$$

$$a_{1,t} = a_{G+1,t} = 0 \quad and \quad c_{n,g,t} > 0 \tag{8}$$

In each period t, if a household is of working age, it earns a wage $W_{n,t}$ by supplying 1 unit of labor inelastically to domestic firms. Households also receive returns on their savings and earn interest based on the savings from the previous period or previous age.

Households face a consumption-saving trade-off, deciding whether to save or borrow in financial markets, with the interest rate $r_{n,t}$ at time t. The amount of savings held by a household of age g, born in period t, and chosen in the prior period, is denoted as $a_{n,g,t+g-1}$. Similarly, households may save an amount $a_{g+1,t+g}$, which will accumulate interest for the next period. Households start with zero assets at age 1 and end with zero assets at age G: $a_{n,1,t} = a_{n,G+1,t} = 0$.

The term $tr^{T}_{n,t} \equiv \dfrac{D_{n,t}}{N_{n,t}}$ refers to trade-related transfers, which are defined as the trade deficit divided by the total population $N_{n,t}$. The term $tr^{D}_{n,t}$ denotes the accidental bequests relevant transfer. The accidental bequests left by households who passed away before age G accidentally between period $t-1$ to t are distributed equally across the total population as a lump-sum transfer, denoted as:[4]

$$tr_{n,t}^{D} \equiv P_{n,I,t}\left(1+r_{n,t}\right)\frac{\sum_{g=2}^{G}\left(N_{n,g-1,t-1}-N_{n,g,t}\right)a_{n,g,t}}{N_{n,t}}. \tag{9}$$

For households aged $g \in [1, G-1]$ born at time t, the intertemporal Euler equation is given by:

$$u'\left(c_{n,g,t+g-1}\right) = \left(\beta s_{n,g+1,t+g}\right)\left(\frac{\psi_{n,t+g}}{\psi_{n,t+g-1}}\right)\frac{\frac{P_{n,I,t+g}}{P_{n,C,t+g}}}{\frac{P_{n,I,t+g-1}}{P_{n,C,t+g-1}}}\left(1+r_{n,t+g}\right)u'\left(c_{n,g+1,t+g}\right). \tag{10}$$

3.3. International trade

Trade is subject to "iceberg" trade costs. One unit of a tradable good in sector j shipped from region i to region n require $\kappa_{ni,t}^{j} \geq 1$ units in i, and the trade cost within region equal to 1, $\kappa_{nn,t}^{j} = 1$. The unit price of an input bundle is given by:

$$c_{n,t}^{j} \equiv \Upsilon_{n}^{j}\left[\left(W_{n,t}\right)^{\beta_{n}^{j}}\left(R_{n,t}\right)^{1-\beta_{n}^{j}}\right]^{\gamma_{n}^{j}}\prod_{k=1}^{J} P_{n,t}^{k\ \gamma_{n}^{k,j}} \tag{11}$$

As in Eaton and Kortum (2002), the fraction of country n's expenditures in sector j goods source from country i is given by:

$$\pi_{ni,t}^{j} = \frac{\lambda_{i,t}^{j}\left(c_{i,t}^{j}\kappa_{ni,t}^{j}\right)^{-\theta}}{\sum_{m=1}^{N}\lambda_{m,t}^{j}\left(c_{m,t}^{j}\kappa_{nm,t}^{j}\right)^{-\theta}}. \tag{12}$$

I abstract international borrowing and lending and model trade imbalances as transfers between countries, following Caliendo, Parro, Rossi-Hansberg, and Sarte (2018). A pre-determined share of GDP, $\phi_{n,t}$ is sent to a global portfolio, which in turn disperses a per-capita lump-sum transfer, T_t^P,to every country. The net transfer or trade deficit, are calculated as:

$$D_{n,t} = -\phi_{n,t}\left(R_{n,t}K_{n,t} + W_{n,t}E_{n,t}N_{n,t}\right) + N_{n,t}T_t^P. \tag{13}$$

3.4. Aggregation and equilibrium condition

3.4.1. Aggregation

Three markets must clear in this model: the labor market, the capital market, and the goods market. Each of these equations amounts to a statement of supply equals demand.

4. Here, the change of the size of individual can either counted as net death ($\eta_{n,g-1,t-1} - \eta_{n,g,t} > 0$) or net immigrant ($\eta_{n,g-1,t-1} - \eta_{n,g,t} < 0$) for country n. For the net death case, I treated it as positive bequests. For the net immigrant case, I assume that the net immigrant (g, t) enter country n with zero assets, and treated it as negative bequests.

Total demand of capital and labor

$$\sum_{j=1}^{J}\int_{0}^{1} l_{n,t}^{j}(\omega)d\omega = N_{n,t}; \quad \sum_{j=1}^{J}\int_{0}^{1} k_{n,t}^{j}(\omega)d\omega = K_{n,t} \tag{14}$$

Define $C_{n,t}$ as aggregate consumption in country n and time t, which is a CES aggregate of sectoral consumption:

$$C_{n,t} \equiv \prod_{j=1}^{J} {C_{n,t}^{j}}^{\alpha_{n,C,t}^{j}}, \text{ where } \sum_{j=1}^{J} \alpha_{n,C,t}^{j} = 1. \tag{15}$$

Similar relation for the aggregate investment and sectoral investment is given by

$$I_{n,t} \equiv \prod_{j=1}^{J} {I_{n,t}^{j}}^{\alpha_{n,I,t}^{j}}, \text{ where } \sum_{j=1}^{J} \alpha_{n,I,t}^{j} = 1. \tag{16}$$

Now, aggregate individual variables across cohorts, I have

$$C_{n,t} \equiv \sum_{g=1}^{G} N_{n,g,t} c_{n,g,t}; \quad K_{n,t} \equiv \sum_{g=2}^{G} N_{n,g-1,t-1} a_{n,g,t}. \tag{17}$$

Aggregating individual budget constraints across ages, along with the equation for accidental bequests, yields the following aggregate-level budget constraint:

$$P_{n,C,t}C_{n,t} + P_{n,I,t}I_{n,t} = (r_{n,t}+\delta) P_{n,I,t}K_{n,t} + L_{n,t}^{e}W_{n,t} + D_{n,t}. \tag{18}$$

Finally, each composite good is used as an intermediate and as final consumption, total expenditure on a composite good in sector j, region n is

$$X_{n,t}^{j} = \alpha_{C,n}^{j} P_{C,n,t} C_{n,t} + \alpha_{I,n}^{j} P_{I,n,t} I_{n,t} + \sum_{k=1}^{J} \gamma_{n}^{j,k} \left(\sum_{i=1}^{N} X_{in,t}^{k} \right). \tag{19}$$

Cost minimization implies that, expenditure on factors exhaust the value of output:

$$W_{n,t}L_{n,t}^{e} = \sum_{j=1}^{J} \beta_{n}^{j}\gamma_{n}^{j} \sum_{i=1}^{N} \pi_{in,t}^{j} X_{i,t}^{j}; \quad R_{n,t}K_{n,t} = \sum_{j=1}^{J} \left(1-\beta_{n}^{j}\right)\gamma_{n}^{j} \sum_{i=1}^{N} \pi_{in,t}^{j} X_{i,t}^{j}. \tag{20}$$

3.4.2. Equilibrium condition

Definition 1: Stationary balanced growth equilibrium A stationary balanced growth competitive equilibrium in the perfect foresight overlapping generations model with G period lived agents, and exogenous population dynamics, is defined as constant allocations of stationary consumption, capital and prices: $\left\{ \{c_{n,g}\}_{g=1,\ n=1}^{G,\ N},\ \{b_{n,g+1}\}_{g=1,\ n=1}^{G-1,N},\ \{W_{n},\ R_{n}\}_{n=1}^{N} \right\}$, satisfies the following conditions: i. The households taking prices transfer and deficit as given, optimize lifetime utility; ii. Firms taking prices as given, minimize production cost; iii. Each country purchases intermediate varieties from the least costly supplier/country subject to the trade cost; iv. All markets are clear; v. The population distribution reaches a stationary steady-state distribution before the economy reaches a steady state.

Definition 2: Dynamics equilibrium Given a set of initial capital distributions and exogenous forces across countries and over time, the transitional dynamics equilibrium (equilibrium transition path) in the perfect foresight overlapping generations trade model with G-period lived agents is defined as allocations of consumption, capital and prices: $\left\{\{c_{n,g}\}_{g=1,\ n=1}^{G,\ N},\ \{b_{n,g+1}\}_{g=1,\ n=1}^{G-1,N},\ \{W_n,\ R_n\}_{n=1}^{N}\right\}_{t=1,\cdots,T+1}$ satisfies the following conditions: i. The households taking prices transfer and deficit as given, optimize lifetime utility; ii. Firms taking prices as given, minimize production cost; iii. Each country purchases intermediate varieties from the least costly supplier/country subject to the trade cost; iv. All markets are clear.

At each point in time, I take world GDP as the numeraire. That means all prices are expressed in units of current world GDP. Table A.1 and Table A.2 in the appendix provide the sets of equilibrium equations for the stationary balanced growth equilibrium and the dynamic equilibrium, respectively.

3.5. How model works

In the model, the main driving forces, age-time varying fertility rates and survival rates, mediated through the model's mechanisms, affect both sectoral productivities and capital accumulations. These forces, together with the exogenous trade cost changes, affect the sectoral prices, which, in turn, affects the allocation of production across sectors and locations, and ultimately affects both trade patterns and economic performance. For example, a higher survival rate leads to greater knowledge stock and capital stock accumulation, raising the balanced growth path by enhancing both productivity and capital. Free trade induce specialization, which encourages higher productivity and lowers prices, ultimately leading to even greater capital accumulation.

In addition, A lower fertility rate impacts both knowledge and capital stocks. In the short run, a reduced young population raises capital per person, temporarily boosting economic output. However, over time, this benefit is offset by slower productivity growth due to the demographic shift, ultimately causing capital per person to fall below the previous growth path.

Trade liberalization can mitigate this long-term drawback by maintaining capital per person above the old growth path for a longer period, which extends the overall economic benefits in comparison to a closed economy scenario.

For a detailed illustration of how the model operates—demonstrated through numerical experiments under both the stationary balanced growth equilibrium and the dynamic transitional equilibrium—please refer to Appendix D.

4. Calibration

In this section, I first calibrate the exogenous, time-invariant parameters, followed by the derivation of time-varying shocks. For the historical shocks over the period 1970–2020, I present their evolution and provide interpretations. These shocks are then fed into the model to assess the accuracy of the calibration. For further details on the calibration procedure, see Appendix B and subsection E.2 in the appendix.

4.1. Time invariant parameters

Households are born with age 1, join the labor market after age $G_0 = 15$, retire after age $G_1 = 65$, and die after age $G = 85$. The annual discount factor is estimated to be $beta = 0.96$, and the annual depreciation rate of capital is $\delta = 0.06$. The coefficient of relative risk aversion is $\sigma = 1$. Following Simonovska and Waugh (2014), I set the trade elasticity $\theta = 4$. The elasticity of substitution between varieties within the composite good plays no quantitative role in the model, I set $\rho = 2$, similar to most trade literature. In the remaining part of this section, I omit the time subscripts t for convenience.

The sectoral expenditure data X_{ni}^j and sectoral value-added data V_n^j are derived from the IO Table. The value of region i's exports of sector j goods to region n is denoted as X_{ni}^j. Similarly, the value of region i's imports of sector j goods from region n is denoted as X_{in}^j. The trade deficit of region n in sector j is defined as $D_n^j = \sum_{i=1}^{N} (X_{ni}^j - X_{ni}^j)$. The aggregate trade deficit of region n is represented as D_n, and it is calculated as $D_n = \sum_{j=1}^{J} D_n^j$. The gross production value of sector j goods in region n is denoted as Y_n^j, and it is computed as $Y_n^j = \sum_{i=1}^{N} X_{in}^j$. The gross expenditure value of sector j goods in region n is denoted as X_n^j, and it is computed as $X_n^j = \sum_{i=1}^{N} X_{ni}^j$. The value added by region n from sector j is V_n^j, and the total value added by region n is denoted as V_n, where $V_n \equiv W_n L_n^e + R_n K_n = \sum_{j=1}^{J} V_n^j$.

Furthermore, the value of demand for sector j goods in region n's production of sector k goods is represented as $V_n^{j,k}$, and the production share parameters can be backed out through:

$$\gamma_n^j = \frac{V_n^j}{Y_n^j}, \qquad \gamma_n^{j,k} = (1 - \gamma_n^j)\frac{V_n^{j,k}}{\sum_{j=1}^{J} V_n^{j,k}}. \tag{21}$$

The preference parameters $\alpha_{C,n}^j$ and investment parameters $\alpha_{I,n}^j$ can be backed out through:

$$\alpha_{C,n}^j = \frac{P_n^j C_n^j}{P_{n,C} C_n}, \alpha_{I,n}^j = \frac{P_n^j I_n^j}{P_{n,I} I_n}, \tag{22}$$

where value of country n's sectoral goods consumption $P_n^j C_n^j$ and value of country n's total consumption $P_{n,C} C_n$ can be got directly from IO table. I then take the average of those parameters which generated from IO table across the years and regions.

4.2. Time varying shocks

4.2.1. Demographics, Labor input, capital and investment

Given the number of age g population for country n at time t, the conditional survival rate, which represents the probability of continuing survival from age g to $g+1$, is defined as $s_{n,g+1,t+1} = \frac{N_{n,g+1,t+1}}{N_{n,g,t}}$. The model does not distinguish between women and men. Therefore, a parsimonious way to define the survival rate is to consider the number of newborn cohorts (age $g = 1$) at time t divided by the population within the fertility age range. The fertility age is defined as individuals between age $g = 21$ and age $g = 49$. Consequently, the fertility rate is calculated as $f_{n,g,t} = \frac{N_{n,g=1,t}}{\sum_{g=21,\cdots,49} N_{n,g,t-1}}, g \in [21, 49]$ and $f_{n,g,t} = 0, g \notin [21, 49]$.

The labor supply denoted as $L_{n,t}$ and human capital (schooling) index are derived directly from PWT 10.01 in Feenstra, Inklaar, and Timmer (2015). The same dataset provides data on capital stock, which I use to calibrate the initial aggregate capital stocks, K_{n,t_1}, in line with my model. Information on aggregate and sectoral investment values ($P_{I,n,t} I_{n,t}$ and $P_{n,t}^j I_{n,t}^j$) is sourced from the World Input-Output Database Timmer, Dietzenbacher, Los, Stehrer, and De Vries (2015); Woltjer, Ggouma, and Timmer (2021). Using sectoral intermediate prices, I calculate the quantities of investment, $I_{n,t}$, and capital stock, $K_{n,t}$.

The total population $N_{n,t}$ and age distribution data $N_{n,g,t}$ are sourced from the United Nations World Population Prospects 2022. Labor market distortions are computed using the formula $\tau_{n,t}^L = 1 - \frac{N_{n,t}}{\bar{L}_{n,t}}$. The trade imbalance shifters $\phi_{n,t}$ are defined as the ratio of net exports to GDP, given by $\phi_{n,t} = -\frac{D_{n,t}}{V_{n,t}}$.

Figure 1 presents the calibrated average fertility rate and unconditional survival rate up to age 65, alongside China's total population and working-age share over time. The fertility rate continues its steady decline after the 1990s, reflecting long-term demographic changes. Meanwhile, the survival rate demonstrates a consistent upward trend across all regions, indicating improvements in life expectancy over time.

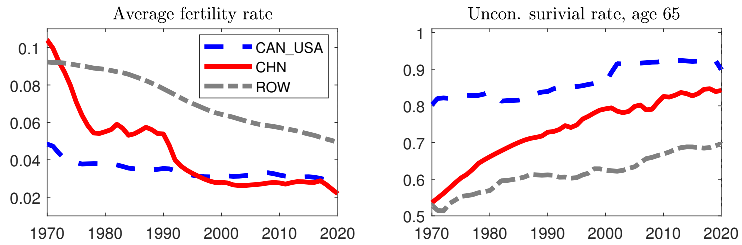

Figure 1
Fertility rate and survival rate

Figure 2 plots labor supply wedges over time. The labor supply wedges reflect various frictions such as female labor force participation, business cycles, and other labor market distortions. Compared to other regions, China's labor supply is less distorted in terms of levels, although it exhibits a declining trend in labor supply after the 1990s, while most other regions show an upward trend.

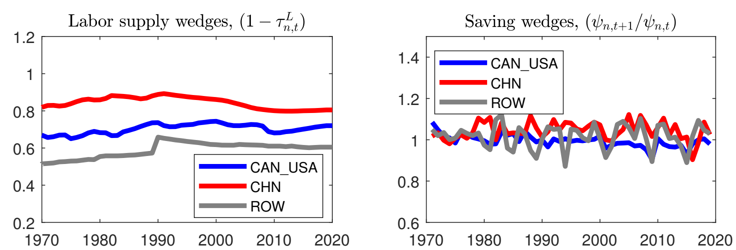

Figure 2
Labor supply wedges and saving wedges

4.2.2. Calibrate saving (or investment) wedges

The saving wedges from 1970 to 2200 are calibrated jointly using the entire period's data (1970–2100). These wedges are used to ensure that the model-generated time-varying aggregate saving (or capital level) matches the real data counterpart. I use the aggregate capital stock, $K_{n,t}$, as targets to calibrate the evolution of saving wedges, $\psi_{n,t}$, over time. For calibration details, please refer to Appendix E.

Figure 2 also plots saving wedges over time. The saving wedges capture forces influencing individuals' saving behavior, aside from demographic factors. Generally, these saving wedges display similar patterns of change across countries, with fluctuations centered around 1.

4.2.3. Knowledge stock and trade cost

Given $W_{n,t}$ and $R_{n,t}$, one can calculate $S^j_{n,t}$ from

$$S^j_{n,t} \equiv \ln\left(\lambda^j_{n,t}\left(c^j_{n,t}\right)^{-\theta}\right),$$

From Equation 12, the trade cost can be derived as follows:

$$\kappa_{ni,t}^{j} = \{ \left(\frac{X_{ni,t}^{j}}{X_{nn,t}^{j}} \right) exp(S_{n,t}^{j} - S_{i,t}^{j}) \}^{-\frac{1}{\theta}}; \tag{23}$$

and the knowledge stock can be derived from:

$$\lambda_{n,t}^{j} = \frac{exp\left(S_{n,t}^{j}\right)}{\left(c_{n,t}^{j}\right)^{-\theta}}. \tag{24}$$

Figure 3 presents the calibrated mean productivity ${\lambda_{n,t}^{j}}^{1/\theta}$ across sectors over time. The productivity levels for the U.S. and Canada region in 1970 are normalized to 1. Overall, China's productivity exhibits an upward trend across all sectors, characterized by a steeper trend compared to other regions, although starting from lower initial levels.

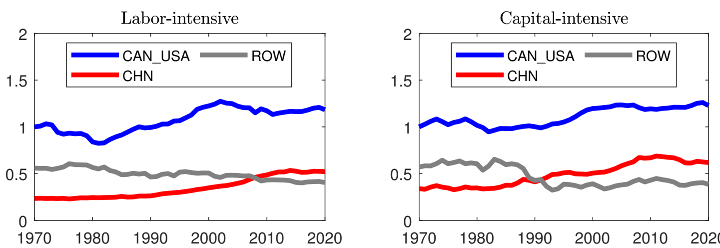

FIGURE 3
KNOWLEDGE STOCKS

Figure 4 depicts the cross-region distribution of average estimated trade costs across each sector over time. It is evident that trade costs generally exhibit a downward trend.

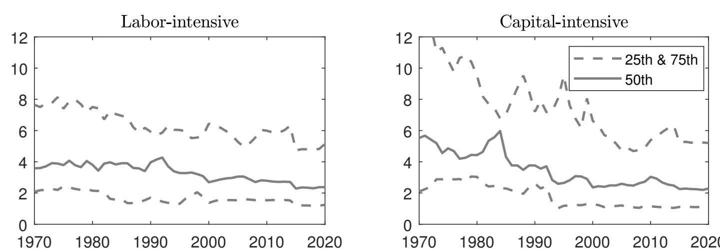

FIGURE 4
TRADE COSTS

4.3. Model fit

To assess the accuracy of the calibration, I reintroduce both the calibrated time-invariant parameters and the time-varying shocks into the model and solve it. Figure 5 presents a comparison between model-generated values (y-axis) and real-world values (x-axis). The data points include the log of total sectoral expenditure, value added, capital, wage rate,

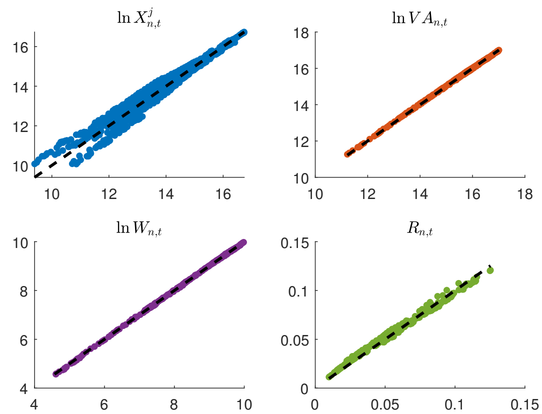

Note: The scatter plots display real data on the x-axis and model-generated values on the y-axis, with a 45-degree reference line on the diagonal.

Figure 5
Calibration Efficiency

and the level of rental rate, and sectoral expenditure share. The correlation between the model-generated and actual data closely aligns with the 45-degree line, indicating that the calibrated shocks successfully replicate real-world patterns.

5. Quantitative Analysis

In this section, I quantify the effects of demographic structures on China's economic growth and trade patterns, as well as to conduct projections for China's future form preservative of demographics.

I explore three counterfactual scenarios. First, I remove both the demographic-induced-saving effects and demographic-induced-productivity changes. Specifically, I replace the age-varying fertility and survival rates in China with those of the rest of the world (RoW) and allow productivity to change in response to changes in demographics. I refer to this as the *without demographic scenario*. Second, I remove only the demographic-induced-saving effects. In this scenario, I again replace China's age-varying fertility and survival rates with those of the RoW but retain the usual productivity changes. I call this the *demographic-capital channel scenario*. Third, I remove only the demographic-induced-productivity effects. In this case, I maintain the original age-varying fertility and survival rates of China and its implied demographic process. I then allow productivity to change as if China's age-varying fertility and survival rates mirror those of the RoW. I refer to this as the *demographic-idea channel scenario*.

5.1. Demographics, economic growth, and trade patterns change

Figure 6 presents time series plots of China's real income per working-age person, represented by solid lines in each subplot. For each variable, I also include its counterparts from each counterfactual scenario, depicted with dotted lines, which represent scenarios where specific forces are muted. This same approach is applied in Figure 7, where I similarly plot the Revealed Comparative Advantage (RCA) index for the capital-intensive sector. To facilitate comparison, I normalize each year's actual data to 1, allowing the dotted counterparts to be interpreted relative to this baseline. I also display these indices in levels, as shown in Figure F.4, and Figure F.5 from appendix.

Demographics and economic growth As shown in Figure 6, if China's fertility and survival rates were equal to those of the ROW, the real income per working-age person in China would be lower relative to the old path, with an increasing gap over time. By 2020, had China's demographic trends mirrored those of the ROW, the real income per working-age person in China would have been about 5.08% less than its actual level.

Two main forces drive these deviations from the historical path: the *Demographic-capital channel* and the *Demographic-idea channel*. As illustrated in Figure 6, the *Demographic-capital channel* pulls real income per working-age individual in China below the historical path. When China's demographic trends align with those of the ROW, its population distribution skews towards higher consumption rather than saving (e.g., a smaller proportion of older working-age individuals or a larger share of younger individuals). This demographic shift reduces capital per working-age person, thereby driving real income per working-age individual below the historical trajectory. By 2020, through the *Demographic-capital channel*, China's real income per working-age person would be about 6.99% lower than observed.

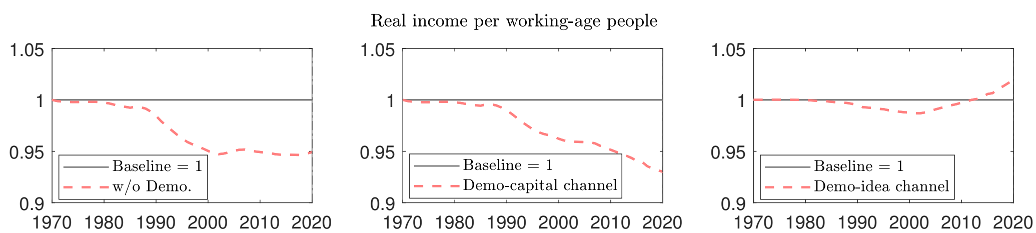

FIGURE 6
REAL INCOME PER WORKING-AGE PEOPLE

Additionally, the *Demographic-idea channel* initially pushes real income per working-age individual below the historical path before pulling it above that path post-2000. When China's demographic trends follow those of the ROW, the working-age population initially falls below the historical path but eventually rises above it. Since the size of the working-age population correlates positively with productivity—given that a larger working-age population generates more ideas—this demographic structure ultimately raises real income per person, or per working-age individual, above the historical path. By 2020, through the *Demographic-idea channel*, real income per working-age individual in China would be about 1.95% higher than the observed level.

In sum, the *Demographic-capital channel* exerts a stronger influence than the *Demographic-idea channel*. Thus, if China's fertility and survival rates had matched those of the ROW, China's transitional path would reflect a lower real income per working-age individual than in its real-world counterpart. As of 2020, this income difference would amount to about 5.08% decrease from observed levels.

Demographics and Trade Pattern Changes Building on the counterfactual exercises previously discussed, I now focus on changes in trade patterns and specialization. I utilize the Revealed Comparative Advantage (RCA) index for the capital-intensive sector to quantify shifts in comparative advantage across sectors.[5]

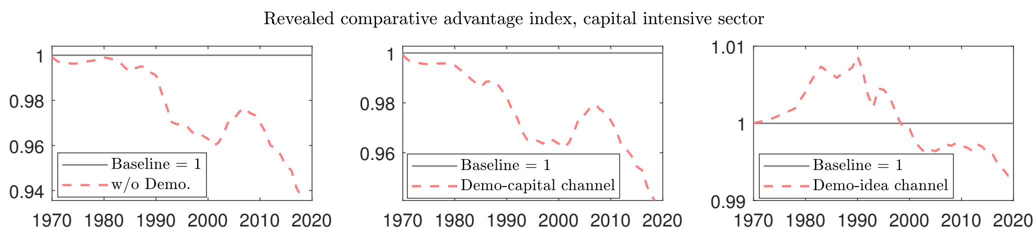

FIGURE 7
REVEALED COMPARATIVE ADVANTAGE INDEX

As shown in Figure 7, if China's fertility and survival rates were aligned with those of the ROW, the RCA index for China's capital-intensive sector would decrease relative to its previous trajectory, with the gap increasing over time. This downward trend implies that, under the RoW similar demographic trends, China's comparative advantage in the capital-intensive sector would decline. Conversely, this shift would indicate a rising comparative advantage in the labor-intensive sector. By 2020, had China's demographics matched those of the RoW, its degree of comparative advantage in the capital-intensive sector would be approximately 6.79% lower than the reality level, implying a stronger comparative advantage in the labor-intensive sector.

Two primary forces drive these deviations from the previous trajectory: the *Demographic-Capital Channel* and the *Demographic-Idea Channel*. As illustrated in Figure 7, the *Demographic-*

5. The Revealed Comparative Advantage (RCA) index, as developed by Balassa (1965), is used here to identify implied comparative advantage forces within each sector. The RCA for the capital-intensive sector is defined as:

$$RCA_{nj} = \left(\frac{Export_{n,j}}{\sum_n Export_{n,j}}\right) / \left(\frac{\sum_j Export_{n,j}}{\sum_{j,n} Export_{n,j}}\right),$$

where n refers to the country, j refers to the sector, and $Export_{n,j}$ denotes the value of country n's sector j exports. A higher RCA_{nj} indicates a greater degree of specialization for country n sector j.

Capital Channel reduces China's comparative advantage in the capital-intensive sector relative to its previous path. Under demographic trends similar to the ROW, China's capital per working-age person would fall below its actual level, thereby implying a lower comparative advantage in the capital-intensive sector. By 2020, the *Demographic-Capital Channel* would have reduced China's comparative advantage in the capital-intensive sector about 6.15% below its actual level, indicating a corresponding increase in the labor-intensive sector's comparative advantage.

From Figure 6, the *Demographic-idea channel* initially drove the RCA index for China's capital-intensive sector above the old path, before pushing it below the old path after the 1990s. As China's demographic trends began to align with those of the ROW, China's working-age population initially fell below the old path, subsequently rising above it. Since the size of the working-age population is positively related to productivity (as a larger working-age cohort generates more ideas), the knowledge stock first trailed below the old path before later exceeding it.

Furthermore, given that sectors differ in their idea duplication coefficient, "φ_j," capital-intensive manufacturing and services sectors, which exhibit relatively lower "φ_j" values, imply a lower elasticity of knowledge stock (or the number of new ideas) with respect to the working-age population. Consequently, despite similar shifts in the working-age population, the variation in the capital-intensive sector will be smaller. Specifically, for the capital-intensive sector, the knowledge stock (productivity) growth rate declines less initially and rises less subsequently, suggesting a higher comparative advantage at the beginning, but a lower advantage thereafter. By 2020, if China's demographic trends had continued to mirror those of the RoW, then through the *Demographic-idea channel*, China's comparative advantage in the capital-intensive sector would be approximately 0.068% lower than in reality.

Overall, the *Demographic-Capital Channel* exerts a greater influence than the *Demographic-Idea Channel*. Thus, if China's fertility and survival rates equaled those of the ROW, China would experience a reduction in comparative advantage in the capital-intensive sector compared to its real-world counterpart along the transition path. By 2020, China's comparative advantage in the capital-intensive sector would be about 6.79% lower than its actual level.

5.2. Model based projection

In this subsection, I analyze how China's demographic trends influence its future economic growth, drawing on the counterfactual exercises presented in the previous section.

Figure 8 displays the time series for the total population, working-age population, and working-age share over an extended period from 1970 to 2070. Assuming an identical initial population distribution, if China's fertility and survival rates were aligned with those of the

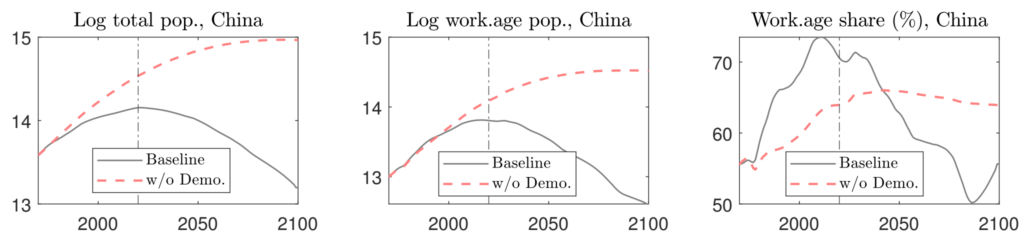

FIGURE 8
DEMOGRAPHIC PROCESS

ROW,[6] China's total population would have been larger than the actual observed levels, with this gap expected to widen over time.

A similar trend can be observed within the working-age population. This demographic shift implies similar patterns for knowledge stock, as a larger working-age population , on average, generates more ideas, thereby contributing to knowledge stock growth. The working-age share, however, presents a contrasting pattern. Initially, this counterfactual share falls below the old path, with the gap gradually widening up to the 2010s. Afterward, however, this gap begins to narrow, with the counterfactual working-age share converging toward the old path around 2040. Beyond the 2040s, the counterfactual share continues to rise, diverging further from the old path.

These demographic shifts suggest analogous trends for the capital stock process. As depicted in Figure 9, regarding capital stock per person, had China's fertility and survival rates aligned with the RoW, the capital stock per person would have experienced a decline and remained below the old path for the entire period from 1970 to 2070. This trend is influenced by variations in population distribution across age groups, as individuals at different life stages tend to save at differing rates. Consequently, an age structure favoring savings leads to an increase in capital stock per working-age person, and vice versa.

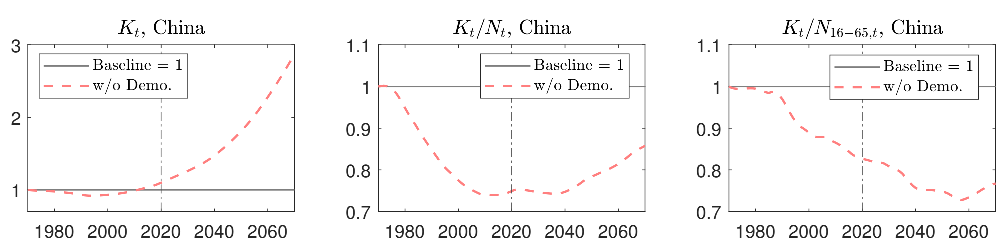

FIGURE 9
CAPITAL STOCKS

Figure 10 presents the time-varying process of China's real income per working-age person, along with its counterfactual counterparts under three aforementioned scenarios. If

6. Overall, this scenario would result in a lower trajectory for China's increasing survival rate and a higher trajectory for China's decreasing fertility rate.

China's fertility and survival rates were to align with those of the ROW, the real income per working-age person in China would be lower relative to the baseline path, with the gap increasing over time. This gap begins to narrow after 2020, and by around 2060, the counterfactual path of real income per worker surpasses the old path.

Two primary forces drive the U-shaped deviations of the counterfactual real income per working-age person from the historical path: the *Demographic-capital channel* and the *Demographic-idea channel*. As illustrated in Figure 9 and Figure 10, the *Demographic-capital channel* pulls the counterfactual real income per working-age person in China below the historical path due to the declining capital stock per working-age person relative to the baseline. The *Demographic-idea channel* has driven the counterfactual real income per working-age person in China above its historical path. If China's fertility rate and survival rate were equal to those of the ROW, it would imply a larger working-age population than in reality. Since the size of the working-age population correlates positively with productivity, the *Demographic-idea channel* leads to higher productivity levels, which in turn raises real income per person above the actual path.

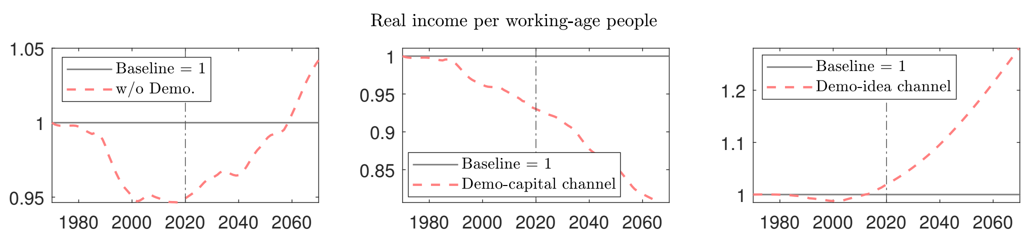

FIGURE 10
REAL INCOME PER WORKING-AGE PEOPLE

These two forces operate in opposite directions, with their relative strengths reversing around the year 2060. This implies that, before 2060, assuming an identical initial population distribution, if China's fertility rate and survival rate were equal to that of the ROW, the *Demographic-capital channel* effects would dominate. The counterfactual demographic structure favors consumption more than the actual demographic structure, which results in a lower capital per worker compared to the baseline, thus leading to a lower real income per worker relative to the baseline. After 2060, the *Demographic-idea channel* effects become larger. The counterfactual demographic structure implies a higher working-age population relative to reality. Since the size of the working-age population is positively correlated with productivity, this results in higher productivity, leading to a higher real income per worker compared to the baseline.

These facts reveal a short-run and long-run trade-off for China's paiticular demographics process compared to that the ROW. If China's fertility rate and survival rate were equal to that of the ROW, in the short run until 2060, the counterfactual demographic structure would imply lower capital stocks per worker, resulting in a lower level of real income per worker. In the long run, after 2060, the counterfactual demographic structure features a higher proportion of the working-age population. This shift would bring more ideas, thereby boosting productivity. As a result, the long-run effect leads to a higher level of real income per worker than in the reality scenario.

6. Conclusion

This paper investigates how demographic forces have shaped China's economic growth and trade patterns, and provides model-based projections for its future growth.

I find that, in the short run, the *demographic-capital channel* exerts a stronger influence than the *demographic-idea channel*. Thus, if China's fertility and survival rates had matched those of the rest of the world, China's counterfactual transitional path would reflect a lower real income per worker than its real-world counterpart. In parallel, China would experience a lower degree of its comparative advantage in the capital-intensive sector compared to its real-world counterpart. By 2020, China's real income per worker would be about 5.08% lower than its actual level, and China's revealed comparative advantage index in the capital-intensive sector would be about 6.79% lower than its actual level. These short-run trends would persist until 2060.

In the long run, the *demographic-idea channel* exerts a stronger influence than the *demographic-capital channel*. After 2060, the counterfactual demographic structure implies a higher working-age population relative to reality. Since the size of the working-age population is positively correlated with productivity, this results in higher productivity, leading to a higher real income per worker compared to the baseline. By 2070, China's real income per worker would be about 4.08% higher than its projected baseline level.

In this framework, demographic structure affects productivity through the proposed idea generation process. However, another potential link between demographic structure and productivity involves incorporating age-dependent productivity would also deserved to try, where the effectiveness of labor varies by age cohort. Additionally, the model currently assumes a financial autarky, with the trade balance being exogenous. Allowing for cross-border capital flows (or cross-border borrowing) would provide further insights into whether demographic structure affects economic growth and trade patterns through cross-border capital flows. Finally, including countries that have not yet experienced population aging as single country, such as India and Vietnam, would provide additional insights into how global demographic transitions shape global production reallocation and their effects on income. I leave these and other exercises for future research.

References

Aksoy, Yunus, Henrique S Basso, Ron P Smith, and Tobias Grasl (2019). Demographic structure and macroeconomic trends. *American Economic Journal: Macroeconomics*, 11(1), 193–222.

Alessandria, George A, Shafaat Y Khan, Armen Khederlarian, Kim J Ruhl, and Joseph B Steinberg (2021). Trade-policy dynamics: Evidence from 60 years of us-china trade. Technical report, National Bureau of Economic Research.

Alvarez, Fernando (2017). Capital accumulation and international trade. *Journal of Monetary Economics*, 91, 1–18.

Alvarez, Fernando E, Francisco J Buera, Robert E Lucas, et al. (2008). Models of idea flows. Technical report, National Bureau of Economic Research.

Alvarez, Fernando E, Francisco J Buera, Robert E Lucas, et al. (2013). Idea flows, economic growth, and trade. Technical report, National Bureau of Economic Research.

Anderson, James E, Mario Larch, and Yoto V Yotov (2020). Transitional growth and trade with frictions: A structural estimation framework. *The Economic Journal*, 130(630), 1583–1607.

Becker, Gary S, Kevin M Murphy, and Robert Tamura (1990). Human capital, fertility, and economic growth. *Journal of political economy*, 98(5, Part 2), S12–S37.

Buera, Francisco J and Ezra Oberfield (2020). The global diffusion of ideas. *Econometrica*, 88(1), 83–114.

Cai, Sheng, Lorenzo Caliendo, Fernando Parro, and Wei Xiang (2022). Mechanics of spatial growth. Technical report, National Bureau of Economic Research.

Caliendo, Lorenzo, Fernando Parro, Esteban Rossi-Hansberg, and Pierre-Daniel Sarte (2018). The impact of regional and sectoral productivity changes on the US economy. *The Review of economic studies*, 85(4), 2042–2096.

Eaton, Jonathan and Samuel Kortum (2002). Technology, geography, and trade. *Econometrica*, 70(5), 1741–1779.

Eaton, Jonathan, Samuel Kortum, Brent Neiman, and John Romalis (2016). Trade and the global recession. *American Economic Review*, 106(11), 3401–3438.

Fan, Jingting (2019). Internal geography, labor mobility, and the distributional impacts of trade. *American Economic Journal: Macroeconomics*, 11(3), 252–288.

Feenstra, Robert C, Robert Inklaar, and Marcel P Timmer (2015). The next generation of the Penn World Table. *American economic review*, 105(10), 3150–3182.

Feyrer, James (2007). Demographics and productivity. *The Review of Economics and Statistics*, 89(1), 100–109.

Feyrer, James (2008). Aggregate evidence on the link between age structure and productivity. *Population and Development Review*, 34, 78–99.

Hanwei, Huang, Ju Jiandong, and Vivian Z Yue (2024). Accounting for the Evolution of Chinas Production and Trade Patterns.

Hao, Tongtong, Ruiqi Sun, Trevor Tombe, and Xiaodong Zhu (2020). The effect of migration policy on growth, structural change, and regional inequality in China. *Journal of Monetary Economics*, 113, 112–134.

Jones, Benjamin F (2010). Age and great invention. *The Review of Economics and Statistics*, 92(1), 1–14.

Kögel, Tomas (2005). Youth dependency and total factor productivity. *Journal of Development Economics*, 76(1), 147–173.

Lindh, Thomas and Bo Malmberg (1999). Age structure effects and growth in the OECD, 1950–1990. *Journal of population Economics*, 12, 431–449.

Liu, Chen and Xiao Ma (2018). China's Export Surge and the New Margins of Trade.

Lucas Jr, Robert E (2009). Ideas and growth. *Economica*, 76(301), 1–19.

Ma, Lin and Yang Tang (2020). Geography, trade, and internal migration in China. *Journal of Urban Economics*, 115, 103181.

Maestas, Nicole, Kathleen J Mullen, and David Powell (2023). The effect of population aging on economic growth, the labor force, and productivity. *American Economic Journal: Macroeconomics*, 15(2), 306–332.

Ravikumar, B, Ana Maria Santacreu, and Michael Sposi (2019). Capital accumulation and dynamic gains from trade. *Journal of International Economics*, 119, 93–110.

Sevilla, Jaypee et al. (2007). Age structure and productivity growth. *Institute for Future Studies working paper*, 10.

Simonovska, I. and M. E. Waugh (2014). The elasticity of trade: Estimates and evidence. In *Journal of International Economics*, pp. 34–50.

Sposi, Michael (2022). Demographics and the evolution of global imbalances. *Journal of Monetary Economics*, 126, 1–14.

Sposi, Michael, Kei-Mu Yi, and Jing Zhang (2021a). Deindustrialization and industry polarization. Technical report, National Bureau of Economic Research.

Sposi, Michael, Kei-Mu Yi, and Jing Zhang (2021b). Trade integration, global value chains, and capital accumulation. *IMF Economic Review*, 69, 505–539.

Timmer, Marcel P, Erik Dietzenbacher, Bart Los, Robert Stehrer, and Gaaitzen J De Vries (2015). An illustrated user guide to the world input–output database: the case of global automotive production. *Review of International Economics*, 23(3), 575–605.

Tombe, Trevor and Xiaodong Zhu (2019). Trade, Migration, and Productivity: A Quantitative Analysis of China. *American Economic Review*, 109.

United Nations, Department of Economic and Population Division (2024). Social Affairs (2024). 024 revision of the United Nations (2024) World Population Prospects (UN).

Werding, Martin (2008). Ageing and productivity growth: are there macro-level cohort effects of human capital?

Werding, Martin et al. (2007). *Ageing, Productivity and Economic Growth: A Macro-level Analysis.* Project on Intergenerational Equity, Inst. of Economic Research ....

Woltjer, Pieter, Reitze Ggouma, and Marcel P Timmer (2021). Long-run World Input-Output Database: Version 1.0.

Appendix A: Equilibrium details

A.1. Equilibrium equations

TABLE A.1
Steady-state conditions

g_n	$N_{n,g,t+1} = (1+g_n)\, N_{n,g,t}$	$\forall n, t \in [T-1, \infty)$
g_{λ^j}	$\lambda^j_{n,t+1} = (1+g_{\lambda^j})\, \lambda^j_{n,t}$; $(1+g_{\lambda^j}) = (1+g_n)^{\frac{\varphi^j}{(1-\rho)}}$; $1+g_{A^j} \equiv (1+g_{\lambda^j})^{1/\theta}$	$\forall n, j, t \in [T, \infty)$
g_ω	$X \in [\frac{W_{n,t}}{P_{n,C,t}}, \frac{ts^T_{n,t}}{P_{C,n,t}}, \frac{ts^D_{n,t}}{P_{n,C,t}}, a_{n,g,t}, c_{n,g,t}]$; $X_{t+1} = (1+g_\omega)\, X_t$; $1+g_\omega = (1+g_{A^j})^{\frac{1}{\beta^j\gamma^j}} = (1+g_{\lambda^j})^{\frac{1}{\beta^j\gamma^j\theta}}$	$\forall n, t \in [T, \infty)$
$g_{rc^j_n}$	$X \in [\frac{c^j_{n,t}}{P^j_{n,t}}]$; $X_{t+1} = \left(1+g_{rc^j_n}\right) X_t$; $1+g_{rc^j_n} = (1+g_\omega)^{\beta^j\gamma^j} = (1+g_{\lambda^j})^{1/\theta}$	$\forall n, t \in [T, \infty)$
g_K	$X \in [C_{n,t}, C^j_{n,t}, I_{n,t}, I^j_{n,t}, K_{n,t}, Y^j_{n,t}, \frac{X^j_{n,t}}{P^j_{n,t}}, \frac{D_{n,t}}{P^j_{n,t}}, \frac{D_{n,t}}{P_{n,Ct}}, \frac{D_{n,t}}{P_{n,I,t}}]$; $X_{t+1} = (1+g_K)\, X_t$; $1+g_K = (1+g_\omega)(1+g_n)$	$\forall n, j, t \in [T, \infty)$
	$1+g_\omega = (1+g_n)^{\frac{\varphi^j}{\theta\beta^j\gamma^j(1-\rho)}}$; $\varphi^j/\varphi^k = \beta^j\gamma^j/\beta^k\gamma^k$; $\varphi^j = \theta(1-\rho)\,\beta^j\gamma^j \frac{\log(1+g_\omega)}{\log(1+g_n)}$;	$\forall n, j$
F0	$\lambda^j_{n,T+1} - \lambda^j_{n,T} = {N_{n,T}}^{\varphi^j} \left(\lambda^j_{n,T}\right)^\rho \left[\sum_g \eta^j_g \bar{N}_{n,g,T}\right]^{\varphi^j} \Gamma(1-\rho)$	$\forall(n)$
H1	$N_{n,T} \equiv \sum_{g=1}^{G} N_{n,g,T}$; $\bar{L}_{n,T} \equiv \sum_{g=G_0+1}^{G} N_{n,g,T}$; $L_{n,T} = \left(1-\tau^L_{n,T}\right) \sum_{g=G_0+1}^{G_1} N_{n,g,T}\, l_g$; $L^e_{n,T} = E_{n,T} L_{n,T}$	$\forall(n)$
H2	$P_{n,C,T} c_{n,g,T} + P_{n,I,T}(1+g_\omega)\, a_{n,g+1,T} = P_{n,I,T}(1+r_{n,T})\, a_{n,g,T} + W_{n,T}\left(1-\tau^L_{n,T}\right) E_{n,T} l_g + tr^D_{n,T} + tr^T_{n,T}$; $g \in [1, G]$	$\forall(n)$
H3	$a_{1,T} = a_{G+1,T} = 0; c_{n,g,T} > 0, \{c_{n,g,T}\}_{g=1}^{G}; \{a_{n,g+1,T}\}_{g=1}^{G-1}$	$\forall(n)$
H4	$tr^T_{n,T} \equiv \frac{D_{n,T}}{N_{n,T}}; tr^D_{n,T} = P_{n,I,T}(1+r_{n,T}) \sum_{g=2}^{G} \left(\frac{\overline{N}_{n,g-1,T}}{1+g_n} - \overline{N}_{n,g,T}\right) a_{n,g,T}$	$\forall(n)$
H4'	$tr^D_{n,T} = tr^{D,1}_{n,T} + tr^{D,2}_{n,T} = P_{n,I,T}(1-\delta) \sum_{g=2}^{G} \left(\frac{\overline{N}_{n,g-1,T}}{1+g_n} - \overline{N}_{n,g,T}\right) a_{n,g,T} + P_{n,I,T}\left(\frac{R_{n,T}}{P_{n,I,T}}\right) \sum_{g=2}^{G} \left(\frac{\overline{N}_{n,g-1,T}}{1+g_n} - \overline{N}_{n,g,T}\right) a_{n,g,T}$	$\forall(n)$
H4"	$P_{n,C,T} c_{n,g,T} + P_{n,I,T} i_{n,g,T} = R_{n,T} a_{n,g,T} + W_{n,T}\left(1-\tau^L_{n,T}\right) E_{n,T} l_g + tr^{D,2}_{n,T} + tr^T_{n,T}$	$\forall(n)$
H4"'	$P_{n,I,T} i_{n,g,T} = P_{n,I,T}(1+g_\omega)\, a_{n,g+1,T} - \left[P_{n,I,T}(1-\delta)\, a_{n,g,T} + tr^{D,1}_{n,T}\right]$	$\forall(n)$
H5	$(1+g_\omega)\, c_{n,g+1,T} = \left[(\beta s_{n,g+1,T})\left(\frac{\psi_{n,g+1,T+1}}{\psi_{n,g,T}}\right)(1+r_{n,T})\right]^\sigma c_{n,g,T}; \forall\ g \in [1, G-1]$	$\forall(n)$
H6	$C_{n,T} \equiv \sum_{g=1}^{G} N_{n,g,T} c_{n,g,T}; K_{n,T} \equiv \sum_{g=2}^{G} \frac{N_{n,g-1,T}}{1+g_n} a_{n,g,T}$	$\forall(n)$
H7	$C_{n,T} \equiv \prod_{j=1}^{J} {C^j_{n,T}}^{\alpha^j_C}; I_{n,T} \equiv \prod_{j=1}^{J} {I^j_{n,T}}^{\alpha^j_I}; P_{n,I,T} = \prod_{j=1}^{J} \left[\frac{P^j_{n,T}}{\alpha^j_I}\right]^{\alpha^j_I}; P_{n,C,T} = \prod_{j=1}^{J} \left[\frac{P^j_{n,T}}{\alpha^j_C}\right]^{\alpha^j_C}$	$\forall(n)$
H8	$P^j_{n,T} I^j_{n,T} = \alpha^j_{I,n} P_{n,I,T} I_{n,T}; P^j_{n,T} C^j_{n,T} = \alpha^j_{C,n} P_{n,C,T} C_{n,T}$	$\forall(n,j)$
F1	$W_{n,T} L^e_{n,T} = \sum_{j=1}^{J} \beta^j \gamma^j \sum_{i=1}^{N} \pi^j_{in,T} X^j_{i,T}; R_{n,T} K_{n,T} = \sum_{j=1}^{J} \left(1-\beta^j\right) \gamma^j \sum_{i=1}^{N} \pi^j_{in,T} X^j_{i,T}$	$\forall(n)$
F2	$r_{n,T} = \frac{R_{n,T}}{P_{n,I,T}} - \delta$	$\forall(n)$
T1	$c^j_{n,T} \equiv \Upsilon^j \left[(W_{n,T})^{\beta^j} (R_{n,T})^{1-\beta^j}\right]^{\gamma^j} \prod_{k=1}^{J} {P^k_{n,T}}^{\gamma^{k,j}}; \Upsilon^j \equiv \gamma^j \beta^{j^{-\gamma^j\beta^j}} \gamma^j \left(1-\beta^j\right)^{-\gamma^j\left(1-\beta^j\right)} \prod_{k=1}^{J} \gamma^{k,j^{-\gamma^{k,j}}}$	$\forall(n,j)$
T2	$P^j_{n,T} = A \cdot \left[\sum_{i=1}^{N} \lambda^j_{i,T} \left(\kappa^j_{ni,T} c^j_{i,T}\right)^{-\theta}\right]^{-\frac{1}{\theta}}; A \equiv \Gamma\left(\frac{1+\theta-\sigma}{\theta}\right)^{\frac{1}{(1-\sigma)}}$	$\forall(n,j)$
T3	$\pi^j_{ni,T} \equiv \frac{X^j_{ni,T}}{\sum_{i=1}^{N} X^j_{ni,T}} = \frac{\lambda^j_{i,t}\left(c^j_{i,t}\kappa^j_{ni,T}\right)^{-\theta}}{\sum_{m=1}^{N} \lambda^j_{m,T}\left(c^j_{m,T}\kappa^j_{nm,T}\right)^{-\theta}} = \lambda^j_{i,T}\left(\frac{A c^j_{i,T}\kappa^j_{ni,T}}{P^j_{n,T}}\right)^{-\theta}$	$\forall(n,i,j)$
T4	$P_{C,n,T} C_{n,T} + P_{I,n,T} I_{n,T} = R_{n,T} K_{n,T} + W_{n,T} E_{n,T} L_{n,T} + D_{n,T} = R_{n,T} K_{n,T} + W_{n,T} L^e_{n,T} + D_{n,T} \equiv IN_{n,T}$	$\forall(n)$
T4'	$P_{n,C,T} C_{n,T} + P_{n,I,T}(1+g_K)\, K_{n,T} = \left(1 + \frac{R_{n,T}}{P_{n,I,T}} - \delta\right) P_{n,I,T} K_{n,T} + W_{n,T} L^e_{n,T} + D_{n,T}$	$\forall(n)$
T5	$(1+g_K)\, K_{n,T} = K_{n,T+1} = I_{n,T} + (1-\delta)\, K_{n,T}; (g_K+\delta)\, K_{n,T} = I_{n,T}$	$\forall(n)$
T6	$\sum_{j=1}^{J}\sum_{i=1}^{N} X^j_{in,T} - \sum_{j=1}^{J}\sum_{i=1}^{N} X^j_{ni,T} = NX_{n,T} = -D_{n,T}$	$\forall(n,j)$
T6'	$X^j_{n,T} = \alpha^j_C P_{C,n,T} C_{n,T} + \alpha^j_I P_{I,n,T} I_{n,T} + \sum_{k=1}^{J} \gamma^{j,k} \left(\sum_{i=1}^{N} X^k_{in,T}\right)$	$\forall(n,j)$
T7	$D_{n,T} = -\phi_{n,T}\left(R_{n,T} K_{n,T} + W_{n,T} L^e_{n,T}\right) + N_{n,T} T^P_T; T^P_T = \frac{\sum_{n=1}^{N} \phi_{n,T}\left(R_{n,T} K_{n,T} + W_{n,T} L^e_{n,T}\right)}{\sum_{n=1}^{N} N_{n,T}}$	$\forall(n)$
T7'	$D_{n,T} = -\phi_{n,T}\left(R_{n,T} K_{n,T} + W_{n,T} L^e_{n,T}\right) + \frac{N_{n,T}}{\sum_{n=1}^{N} N_{n,T}} \sum_{n=1}^{N} \phi_{n,T}\left(R_{n,T} K_{n,T} + W_{n,T} L^e_{n,T}\right)$	$\forall(n)$

TABLE A.2

Dynamic equilibrium conditions

I1	$\lambda^j_{n,t+1} - \lambda^j_{n,t} = \left(\lambda^j_{n,t}\right)^{\rho} \left(\sum_g \eta^j_g N_{n,g,t}\right)^{\varphi^j} \Gamma\left(1-\rho\right) = N_{n,t}{}^{\varphi^j} \left(\lambda^j_{n,t}\right)^{\rho} \left(\sum_g \eta^j_g \bar{N}_{n,g,t}\right)^{\varphi^j} \Gamma\left(1-\rho\right)$	$\forall(n,t)$
H1	$N_{n,t} \equiv \sum_{g=1}^{G} N_{n,g,t};\ \bar{L}_{n,t} \equiv \sum_{g=G_0+1}^{G} N_{n,g,t};\ L_{n,t} = \left(1-\tau^L_{n,t}\right) \sum_{g=G_0+1}^{G_1} N_{n,g,t} l_g = \left(1-\tau^L_{n,t}\right) \sum_{g=1}^{G} N_{n,g,t} l_g;\ L^e_{n,t} = E_{n,t} L_{n,t}$	$\forall(n,t)$
H2	$P_{n,C,t} c_{n,g,t} + P_{n,I,t} a_{n,g+1,t+1} = P_{n,I,t}\left(1+r_{n,t}\right) a_{n,g,t} + W_{n,t}\left(1-\tau^L_{n,t}\right) E_{n,t} l_g + tr^D_{n,t} + tr^T_{n,t}\ ;\ g \in [1,G]$	$\forall(n,t)$
H3	$a_{1,t} = a_{G+1,t} = 0;\ c_{n,g,t} > 0,\ \left\{c_{n,g,t+g-1}\right\}_{g=1}^{G};\ \left\{a_{n,g+1,t+g}\right\}_{g=1}^{G-1}$	$\forall(n,t)$
H4	$tr^T_{n,t} \equiv \frac{D_{n,t}}{N_{n,t}};\ tr^D_{n,t} \equiv P_{n,I,t}\left(1+r_{n,t}\right) \frac{\sum_{g=2}^{G}\left(N_{n,g-1,t-1} - N_{n,g,t}\right) a_{n,g,t}}{N_{n,t}}$	$\forall(n,t)$
H4’	$tr^D_{n,t} = tr^{D,1}_{n,t} + tr^{D,2}_{n,t} = P_{n,I,t}\left(1-\delta\right) \sum_{g=2}^{G} \left(\frac{N_{n,g-1,t-1} - N_{n,g,t}}{N_{n,t}}\right) a_{n,g,t} + P_{n,I,t} \left(\frac{R_{n,t}}{P_{n,I,t}}\right) \sum_{g=2}^{G} \left(\frac{N_{n,g-1,t-1} - N_{n,g,t}}{N_{n,t}}\right) a_{n,g,t}$	$\forall(n)$
H4”	$P_{n,C,t} c_{n,g,t} + P_{n,I,t} i_{n,g,t} = R_{n,t} a_{n,g,t} + W_{n,t}\left(1-\tau^L_{n,t}\right) E_{n,t} l_g + tr^{D,2}_{n,t} + tr^T_{n,t}$	$\forall(n)$
H4”’	$P_{n,I,t} i_{n,g,t} = P_{n,I,t} a_{n,g+1,t+1} - \left[P_{n,I,t}\left(1-\delta\right) a_{n,g,t} + tr^{D,1}_{n,t}\right]$	$\forall(n)$
H5	$\frac{c_{n,g+1,t+1}}{c_{n,g,t}} = \left[\left(\beta s_{n,g+1,t+1}\right) \left(\frac{\psi_{n,t+1}}{\psi_{n,t}}\right) \frac{\frac{P_{n,I,t+1}}{P_{n,C,t+1}}}{\frac{P_{n,I,t}}{P_{n,C,t}}} \left(1+r_{n,t+1}\right)\right]^{\sigma}\ ;\forall\ g \in [1, G-1]$	$\forall(n,t)$
H6	$C_{n,t} \equiv \sum_{g=1}^{G} N_{n,g,t} c_{n,g,t};\ K_{n,t} \equiv \sum_{g=2}^{G} N_{n,g-1,t-1} a_{n,g,t}$	$\forall(n,t)$
H7	$C_{n,t} \equiv \prod_{j=1}^{J} C^j_{n,t}{}^{\alpha^j_{n,C,t}};\ I_{n,t} \equiv \prod_{j=1}^{J} I^j_{n,t}{}^{\alpha^j_{n,I,t}};\ P_{n,I,t} = \prod_{j=1}^{J} \left[\frac{P^j_{n,t}}{\alpha^j_{I,n}}\right]^{\alpha^j_{I,n}};\ P_{n,C,t} = \prod_{j=1}^{J} \left[\frac{P^j_{n,t}}{\alpha^j_{C,n}}\right]^{\alpha^j_{C,n}}$	$\forall(n,t)$
H8	$P^j_{n,t} I^j_{n,t} = \alpha^j_{I,n} P_{n,I,t} I_{n,t};\ P^j_{n,t} C^j_{n,t} = \alpha^j_{C,n} P_{n,C,t} C_{n,t}$	$\forall(n,j,t)$
F1	$W_{n,t} L^e_{n,t} = \sum_{j=1}^{J} \beta^j_n \gamma^j_n \sum_{i=1}^{N} \pi^j_{in,t} X^j_{i,t};\ R_{n,t} K_{n,t} = \sum_{j=1}^{J} \left(1-\beta^j_n\right) \gamma^j_n \sum_{i=1}^{N} \pi^j_{in,t} X^j_{i,t}$	$\forall(n,t)$
F2	$r_{n,t} = \frac{R_{n,t}}{P_{n,I,t}} - \delta$	$\forall(n,t)$
T1	$c^j_{n,t} \equiv \Upsilon^j_n \left[\left(W_{n,t}\right)^{\beta^j_n} \left(R_{n,t}\right)^{1-\beta^j_n}\right]^{\gamma^j_n} \prod_{k=1}^{J} P^k_{n,t}{}^{\gamma^{k,j}_n}$ where $\Upsilon^j_n \equiv \gamma^j_n \beta^j_n{}^{-\gamma^j_n \beta^j_n} \gamma^j_n \left(1-\beta^j_n\right)^{-\gamma^j_n\left(1-\beta^j_n\right)} \prod_{k=1}^{J} \gamma^{k,j}_n{}^{-\gamma^{k,j}_n}$	$\forall(n,j,t)$
T2	$P^j_{n,t} = A^j \cdot \left[\sum_{i=1}^{N} \lambda^j_{i,t} \left(\kappa^j_{ni,t} c^j_{i,t}\right)^{-\theta}\right]^{-\frac{1}{\theta}}$ where $A^j \equiv \Gamma\left(\frac{1+\theta-\sigma}{\theta}\right)^{\frac{1}{(1-\sigma)}}$	$\forall(n,j,t)$
T3	$\pi^j_{ni,t} \equiv \frac{X^j_{ni,t}}{\sum_{i=1}^{N} X^j_{ni,t}} = \frac{\lambda^j_{i,t}\left(c^j_{i,t}\kappa^j_{ni,t}\right)^{-\theta}}{\sum_{m=1}^{N} \lambda^j_{m,t}\left(c^j_{m,t}\kappa^j_{nm,t}\right)^{-\theta}} = \lambda^j_{i,t} \left(\frac{A^j c^j_{i,t} \kappa^j_{ni,t}}{P^j_{n,t}}\right)^{-\theta}$	$\forall(n,i,j,t)$
T4	$P_{n,C,t} C_{n,t} + P_{n,I,t} I_{n,t} = R_{n,t} K_{n,t} + W_{n,t} E_{n,t} L_{n,t} + D_{n,t} = R_{n,t} K_{n,t} + W_{n,t} L^e_{n,t} + D_{n,t} \equiv IN_{n,t}$	$\forall(n,t)$
T4’	$P_{n,C,t} C_{n,t} + P_{n,I,t} K_{n,t+1} = \left(1 + \frac{R_{n,t}}{P_{n,I,t}} - \delta\right) P_{n,I,t} K_{n,t} + W_{n,t} L^e_{n,t} + D_{n,t}$	$\forall(n,t)$
T5	$K_{n,t+1} = I_{n,t} + \left(1-\delta\right) K_{n,t}$	$\forall(n,t)$
T6	$\sum_{j=1}^{J} \sum_{i=1}^{N} X^j_{in,t} - \sum_{j=1}^{J} \sum_{i=1}^{N} X^j_{ni,t} = NX_{n,t} = -D_{n,t}$	$\forall(n,j,t)$
T6’	$X^j_{n,t} = \alpha^j_{C,n} P_{C,n,t} C_{n,t} + \alpha^j_{I,n} P_{I,n,t} I_{n,t} + \sum_{k=1}^{J} \gamma^{j,k}_n \left(\sum_{i=1}^{N} X^k_{in,t}\right)$	$\forall(n,j,t)$
T7	$D_{n,t} = -\phi_{n,t}\left(R_{n,t} K_{n,t} + W_{n,t} L^e_{n,t}\right) + N_{n,t} T^P_t\ ;\ T^P_t = \frac{\sum_{n=1}^{N} \phi_{n,t}\left(R_{n,t} K_{n,t} + W_{n,t} L^e_{n,t}\right)}{\sum_{n=1}^{N} N_{n,t}}$	$\forall(n,t)$
T7’	$D_{n,t} = -\phi_{n,t}\left(R_{n,t} K_{n,t} + W_{n,t} L^e_{n,t}\right) + \frac{N_{n,t}}{\sum_{n=1}^{N} N_{n,t}} \sum_{n=1}^{N} \phi_{n,t}\left(R_{n,t} K_{n,t} + W_{n,t} L^e_{n,t}\right)$	$\forall(n,t)$

Appendix B: Empirical analysis

Summary statistics

TABLE B.1
Decriptive statistics: 1975 - 2019, 76 countries

VARIABLES	N	mean	sd	between.sd	within.sd	min	max	skewness	kurtosis
Child share	3,420	0.303	0.109	0.10113	0.04205	0.116	0.523	0.155	1.655
Working age share	3,420	0.615	0.0661	0.05784	0.03260	0.457	0.785	-0.366	2.103
Elderly share	3,420	0.0824	0.0532	0.05046	0.01787	0.0167	0.293	0.727	2.447
Dependence ratio	3,420	0.647	0.188	0.16511	0.09093	0.273	1.189	0.672	2.363
Young dependence ratio	3,420	0.518	0.242	0.22284	0.09830	0.158	1.144	0.485	1.947
Old dependence ratio	3,420	0.129	0.0773	0.07303	0.02675	0.0314	0.499	0.880	3.010
TFP growth (%)	3,116	-0.0566	2.211	0.73687	2.08662	-19.36	20.61	-0.620	14.92
Final consumption (% of GDP)	3,285	77.31	11.08	9.53507	5.83873	11.61	148.5	-0.350	5.486
Gross capital formation (% of GDP)	3,284	24.14	7.148	5.03478	5.23456	1.525	89.38	1.437	9.718
Trade cost	3,286	3.181	0.940	0.86371	0.42245	1.174	10.49	1.550	8.612
(K/L) growth (%)	3,116	2.478	2.744	1.93121	1.96096	-5.326	14.27	0.716	4.643
log(K/L)	3,420	10.58	1.417	1.36937	0.39737	5.859	12.87	-0.546	2.613
GDP per capita at constant 2015 price	3,266	15,711	18,828	18,136.57	6,168.70	165.9	112,418	1.715	6.261

B.1. Data description

I used panel data for 76 countries at different income levels, covering the period from 1975 to 2019. The selection of country groups and periods for analysis was based on the availability of data. The data were constructed from various sources, including the United Nations, World Population Prospects report, World Development Indicators database, Penn World Table 10.01, and CEPII database. The specifics of the data sources are listed in Table B.3.

TABLE B.2
Country Group

Income Group	Countries	Num.
High income	Australia, Austria, Belgium, Barbados, Canada, Switzerland, Chile, Cyprus, Germany, Denmark, Spain, Finland, France, United Kingdom, China (Hong Kong SAR), Greece, Ireland, Iceland, Israel, Italy, Japan, Republic of Korea, Luxembourg, Malta, Netherlands, Norway, New Zealand, Panama, Portugal, Romania, Singapore, Sweden, Uruguay, United States of America	34
Upper middle income	Brazil, Botswana, China, Colombia, Costa Rica, Dominican Republic, Jamaica, Jordan, Mexico, Mauritius, Malaysia, Namibia, Peru, Paraguay, Thailand, Ecuador, Gabon, Guatemala, Türkiye, South Africa, Venezuela (Bolivarian Republic of)	21
Lower middle income	Bolivia (Plurinational State of), Côte d'Ivoire, Cameroon, Egypt, Indonesia, India, Iran (Islamic Republic of), Kenya, Sri Lanka, Morocco, Nigeria, Philippines, Senegal, Tunisia, Tanzania, Zimbabwe	16
Lower income	Burkina Faso, Mozambique, Niger, Rwanda, Zambia	5

Notes: According to United Nations list of countries classified by income level

TABLE B.3
DEFINITIONS OF VARIABLES AND DATA SOURCES.

Variables	Description and Construction	Source
Population at every 5 year cohorts	Population at every 5 year cohorts: $[0,4], [5,9], \ldots, [90,94], [95,99]$ and $[100,+]$, 1975-2019	UN, World Population Prospects, 2022 version.
Real GDP per capita	Real GDP per capita at constant 2015 prices (in US $), 1975-2019	World Development Indicators
Gross capital formation (% of GDP)	Gross capital formation (% of GDP), 1975-2019	World Development Indicators
Final consumption expenditure (% of GDP)	Final consumption expenditure (% of GDP), 1975-2019	World Development Indicators
Capital Stock	Capital Stock at constant 2017 prices (in millions US $), 1975-2019	Penn World Table 10.01
Population	Total population (in millions US $), 1975-2019	Penn World Table 10.01
Total factor productivity (TFP)	Total factor productivity (TFP), 1975-2019	Penn World Table 10.01
Gross Domestic Products	Destination and origin country GDP at current prices (in thousands US $), 1975-2019	CEPII
Trade flow	Trade flows as reported by the destination at current prices (in thousands US $), 1975-2019	CEPII

B.2. Other panel regression results

TABLE B.4
THE EFFECT OF DEMOGRAPHIC STRUCTURE ON TECHNOLOGY CHANGE

	Average value in the future 4 years		
VARIABLES	TFP growth rate	Patent.Applications (per 1000 people)	Industrial.Design.Applications (per 1000 people)
Work.Share	11.43***	1.53***	1.36***
(15-64)/ToT	(3.33)	(3.12)	(4.78)
Initial.Log	-3.09***		
.Dependent	(-4.82)		
Constant	20.96***	-0.92***	-0.76***
	(3.65)	(-3.06)	(-4.39)
Observations	732	395	215
R-squared	0.259	0.826	0.913
Time FE	YES	YES	YES
Country FE	YES	YES	YES

Notes: Robust t-statistics in parentheses. *** $p < 0.01$, ** $p < 0.05$, * $p < 0.1$. The variable $Work.Share$ represents the working age share, which is defined as the share of people aged 15-64. The variable $Child.Share$ represents the young population share, which is defined as the share of people aged 0-14, and the variable $Old.Share$ represents old population share, which is defined as the share of people aged 65 and above.

B.3. Robust Checks

For the purpose of conducting robust checks, I performed the same regression analysis by dividing the entire period of 1980–2019 into five 8-year sub-periods: period 1 (1980–1987), period 2 (1988–1995), period 3 (1996–2003), period 4 (2004–2011), and period 5 (2012–2019).

B.3.I. Demographics, technology change, and macroeconomic outcomes

TABLE B.5

THE EFFECT OF DEMOGRAPHIC STRUCTURE

	Average value in the future 7 years					
	Δ TFP/TFP		Cap.F.(% GDP)		Cons.(% GDP)	
Work.Share (15-64)/ToT	8.31***		27.58*		-27.48	
	(2.76)		(1.91)		(-1.61)	
Child.Share (0-14)/ToT		-9.41***		-24.21		27.63
		(-2.80)		(-1.57)		(1.63)
Old.Share (65+)/ToT		-1.02		-66.88**		25.77
		(-0.14)		(-2.47)		(0.62)
Constant	20.69***	30.42***	5.36	34.61***	94.86***	67.45***
	(3.53)	(4.56)	(0.64)	(6.32)	(9.42)	(9.08)
Observations	439	439	431	431	432	432
R-squared	0.367	0.370	0.627	0.633	0.794	0.794
Time FE	YES	YES	YES	YES	YES	YES
Country FE	YES	YES	YES	YES	YES	YES

Notes: Robust t-statistics in parentheses. *** $p < 0.01$, ** $p < 0.05$, * $p < 0.1$. The variable *Dep.Ratio* represents the dependency ratio, which is defined as the ratio of people aged (0-14) and (65, +) to people aged 15-64. The variable $Work.Share$ represents the working age share, which is defined as the share of people aged 15-64. The variable $Child.Share$ represents the young population share, which is defined as the share of people aged 0-14, and the variable *Old.Share* represents old population share, which is defined as the share of people aged 65 and above.

APPENDIX C: MULTI-SECTOR OPEN ECONOMY MODEL DETAILS

C.1. Model details and/or equation derivations

C.1.I. Financial market

The financial market received deposits of $a_{n,g,t}P_{n,I,t}$ from individuals, and must repay those individuals an amount $a_{n,g,t}\left(1+r_{n,t}\right)P_{n,I,t}$. The financial market loaned an amount $K_{n,t} = \sum_{g=2}^{G} N_{n,g-1,t-1}a_{n,g,t}$ to firms to use in production, and from financial intermediate, households receives an amount $\left(1+\frac{R_{n,t}}{P_{n,I,t}}-\delta\right)P_{n,I,t}K_{n,t}$, where note that we have incorporated the fact that some of the capital depreciates in use, and so the total amount returned to the financial market is smaller by this amount. To clear the market it must be that these amounts are equal

$$\sum_{g=2}^{G} N_{n,g-1,t-1}a_{n,g,t}\left(1+r_{n,t}\right)P_{n,I,t} = \left(1+\frac{R_{n,t}}{P_{n,I,t}}-\delta\right)P_{n,I,t}K_{n,t}$$

and as this is a financial autarky economy, the total assets in the economy must be equal to the total capital stock $K_{n,t} = \sum_{g=2}^{G} N_{n,g-1,t-1} a_{n,g,t}$, What this implies is that

$$r_{n,t} = \frac{R_{n,t}}{P_{n,I,t}} - \delta$$

C.1.II. Age structure

The implied unconditional probability of surviving g periods up to time t is given by:

$$S_{g,t} = \prod_{k=1}^{g} s_{k,t+k-g}$$

The unconditional probability of people dying at age g at time t is:

$$D_{g,t} = S_{g-1,t-1}(1 - s_{g,t}) = S_{g-1,t-1} - S_{g,t}$$

The expected life expectancy for people born at t is:

$$\bar{g}_t = \sum_{k=1}^{G} k \cdot D_{k,t+k-1} \quad (1)$$

At time t, if the demographic process reaches a steady state or a balance growth path, the proportion of individuals aged g remains constant, denoted by $\tilde{N}_{n,g}$. Therefore, the population at age g in period t can be expressed as:

$$N_{n,g,t} = \tilde{N}_{n,g} N_{n,t} \tag{C.1}$$

The demographic process can be describe as:

$$N_{1,t+1} = s_{1,t} \sum_{g=1}^{G} f_{g,t} N_{g,t},$$

$$N_{g+1,t+1} = s_{g+1,t+1} N_{g,t}.$$

or

$$\begin{bmatrix} N_{1,t+1} \\ \vdots \\ N_{g,t+1} \\ \vdots \\ N_{G,t+1} \end{bmatrix} = \begin{bmatrix} s_{1,t+1} f_{1,t} & \cdots & s_{1,t+1} f_{g,t} & \cdots & s_{1,t+1} f_{G,t} \\ s_{2,t+1} & 0 & 0 & \cdots & 0 \\ 0 & s_{g+1,t+1} & 0 & \cdots & 0 \\ 0 & \vdots & \vdots & \ddots & \vdots \\ 0 & 0 & s_{G-1,t+1} & \cdots & 0 \\ 0 & 0 & 0 & s_{G,t+1} & 0 \end{bmatrix} \cdot \begin{bmatrix} N_{1,t} \\ \vdots \\ N_{g,t} \\ \vdots \\ N_{G,t} \end{bmatrix}.$$

or $N_t = \Omega_t N_t$.

C.1.III. Other algebra

Now, aggregate individual variables across cohorts, I have:

$$C_{n,t} \equiv \sum_{g=1}^{G} N_{n,g,t} c_{n,g,t} \qquad K_{n,t} \equiv \sum_{g=2}^{G} N_{n,g-1,t-1} a_{n,g,t} \tag{D.1}$$

$$P_{n,C,t} c_{n,g,t} + P_{n,I,t} a_{n,g+1,t+1} = P_{n,I,t}(1+r_{n,t}) a_{n,g,t} + W_{n,t}\left(1-\tau_L^n\right) E_{n,t} l_g + ts_{n,t}^D + ts_{n,t}^T$$

$$ts_{n,t}^D \equiv P_{n,I,t}(1+r_{n,t}) \frac{\sum_{g=2}^{G} (N_{n,g-1,t-1} - N_{n,g,t}) a_{n,g,t}}{N_{n,t}} \tag{D.2}$$

Aggregating individual budget constraints across ages, the budget constraint at the aggregate level is

$$P_{n,C,t} \sum_{g=1}^{G} N_{n,g,t} c_{n,g,t} + P_{n,I,t} \sum_{g=1}^{G} N_{n,g,t} a_{n,g+1,t+1} = P_{n,I,t}(1+r_{n,t}) \sum_{g=1}^{G} N_{n,g,t} a_{n,g,t} \tag{D.3}$$

$$+ \sum_{g=1}^{G} N_{n,g,t} W_{n,t}\left(1-\tau_L^n\right) E_{n,t} l_g + \sum_{g=1}^{G} N_{n,g,t} ts_{n,t}^D + \sum_{g=1}^{G} N_{n,g,t} ts_{n,t}^T \tag{D.4}$$

$$P_{n,C,t} C_{n,t} + P_{n,I,t} K_{n,t+1} = L_{n,t} E_{n,t} W_{n,t} + (1+r_{n,t}) P_{n,I,t} \sum_{g=1}^{G} N_{n,g,t} a_{n,g,t} \tag{D.5}$$

$$+(1+r_{n,t}) P_{n,I,t} \sum_{g=2}^{G} \left(N_{n,g-1,t-1} - N_{n,g,t}\right) a_{n,g,t} + D_{n,t} \tag{D.6}$$

$$= (1+r_{n,t}) P_{n,I,t} K_{n,t} + L_{n,t} E_{n,t} W_{n,t} + D_{n,t} \tag{D.7}$$

$$= \left(1 + \frac{R_{n,t}}{P_{n,t}} - \delta\right) P_{n,I,t} K_{n,t} + L_{n,t}^e W_{n,t} + D_{n,t} \tag{D.8}$$

Aggregate investment can be calculated from

$$I_t \equiv K_{t+1} - (1-\delta) K_t \tag{D.9}$$

Which implies:

$$P_{n,C,t} C_{n,t} + P_{n,I,t} I_{n,t} = (r_{n,t} + \delta) P_{n,I,t} K_{n,t} + L_{n,t}^e W_{n,t} + D_{n,t} \tag{D.10}$$

$$= R_{n,t} K_{n,t} + L_{n,t}^E W_{n,t} + D_{n,t} \tag{D.11}$$

C.2. Computational algorithm

C.2.I. Algorithm to Compute the Steady-state

Algorithm 1 Open Economy Steady State

1: Guess a vector of capital stocks $K^i = \{K_1, \ldots, K_N\}^i$. Then calculate investment $I^i = \{I_1, \ldots, I_N\}^i$, through T5: $I_n = (g_K + \delta)K_n,\ \forall n$.
2: Solve the multi-sector (capital and labor as inputs with different share across sectors) trade model under fixed world GDP, through T1 to T7 and F1, F2, H1, H8, get $\{\pi^j_{ni}, P^j_n, P_n, I_n, P_{n,C}, R_n, W^j_n\}$, $\forall n, i$.
3: Solve $(G-1)$ Euler equations for each Country n, through H2, H3, H4, H5, get a vector of capital stocks

$$\{a^1_{n,1} = a^1_{n,G+1} = 0,\ \{a^1_{n,g+1}\}_{g=1}^{G-1}\}$$

4: Calculate $K^{1'}_n = \sum_{g=2}^{G} \frac{N_{n,g-1}}{1+g_n} a^1_{n,g}$, through H6 for each Country n.
5: Check error term, if $\|K^i - K^{i'}\| < \epsilon$, stop. Else, go to next step.
6: Go back to step 2 with updated new guess K^{i+1}:

$$K^{i+1} = \zeta K^{i'} + (1-\zeta)K^i \quad \text{where } \zeta \in (0,1)$$

C.2.I.1 Detail for Step 3 :

$$\frac{(1+g_\omega)c_{n,g+1,T}}{c_{n,g,T}} = \left[\beta\left(\frac{s_{n,g+1,T+1}\psi_{n,g+1,T+1}}{s_{n,g,T}\psi_{n,g,T}}\right)\left(1+\frac{R_{n,T}}{P_{n,I,T}}-\delta\right)\right]^\sigma$$

$$\frac{(1+g_\omega)c_{n,g+1}}{c_{n,g}} = \left[\beta\left(\frac{s_{n,g+1}\psi_{n,g+1}}{s_{n,g}\psi_{n,g}}\right)(1+r_n)\right]^\sigma = [\beta S_{n,g+1}\Theta_n]^\sigma$$

Define $\Theta_n \equiv 1 + \frac{R_n}{P_{n,I}} - \delta = 1 + r_n$, $G_\omega \equiv 1 + g_\omega$, $S_{n,g+1} \equiv s_{n,g+1}\frac{\psi_{n,g+1}}{\psi_{n,g}}$.
Thus

$$P_{n,C}c_{n,g} = G_\omega \left(\beta S_{n,g+1}\Theta_n\right)^{-\sigma} P_{n,C}c_{n,g+1}$$

Define $\Lambda_{n,g+1} \equiv G_\omega \left(\beta S_{n,g+1}\Theta_n\right)^{-\sigma}$, thus

$$P_{n,C}c_{n,g} = G_\omega \left(\beta S_{n,g+1}\Theta_n\right)^{-\sigma} P_{n,C}c_{n,g+1} = \Lambda_{n,g+1}P_{n,C}c_{n,g+1}$$

From

$$P_{n,C}c_{n,g} = P_{n,I}(1+r_n)a_{n,g} - P_{n,I}(1+g_\omega)a_{n,g+1} + W_n\left(1-\tau^n_L\right)E_n l_g + ts^D_n + ts^T_n$$

and

$$P_{n,C}c_{n,g+1} = P_{n,I}(1+r_n)a_{n,g+1} - P_{n,I}(1+g_\omega)a_{n,g+2} + W_n\left(1-\tau_L^n\right)E_n l_{g+1} + ts_n^D + ts_n^T$$

I have

$$\begin{aligned} &P_{n,I}\Theta_n a_{n,g} - P_{n,I}G_\omega a_{n,g+1} + W_n\left(1-\tau_L^n\right)E_n l_g + ts_n^D + ts_n^T \\ &= \Lambda_{n,g+1}\left[P_{n,I}\Theta_n a_{n,g+1} - P_{n,I}G_\omega a_{n,g+2} + W_n\left(1-\tau_L^n\right)E_n l_{g+1} + ts_n^D + ts_n^T\right] \end{aligned}$$

or

$$\begin{aligned} &P_{n,I}\Theta_n a_{n,g} - \left[\Lambda_{n,g+1}\Theta_n + G_\omega\right]P_{n,I}a_{n,g+1} + \Lambda_{n,g+1}G_\omega P_{n,I}a_{n,g+2} \\ &= W_n\left(1-\tau_L^n\right)E_n\left[\Lambda_{n,g+1}l_{g+1} - l_g\right] + ts_n^T\left[\Lambda_{n,g+1}-1\right] + ts_n^D\left[\Lambda_{n,g+1}-1\right] \end{aligned} \tag{D.14}$$

where

$$\begin{aligned} ts_n^D &\equiv P_{n,I,T}(1+r_{n,T})\sum_{g=2}^{G}\left(\frac{\bar{N}_{n,g-1,T}}{1+g_n} - \bar{N}_{n,g,T}\right)a_{n,g,T} \\ &= P_{n,I}\Theta_n\sum_{g=2}^{G}\left(\frac{\bar{N}_{n,g-1}}{1+g_n} - \bar{N}_{n,g}\right)a_{n,g} \\ &= P_{n,I}\Theta_n \odot \left\{\bar{N}_{n,g-1}(1:G-1,1)./(1+g_n) - \bar{N}_{n,g}(2:G,1)\right\}' \times \bar{a}_n \end{aligned}$$

and

$$ts_n^T \equiv \frac{D_{n,T}}{N_{n,T}}; \quad D_n = -\phi_n\left(R_nK_n + W_nL_n^e\right) + \frac{N_n}{\sum_{n=1}^{N}N_n}\sum_{n=1}^{N}\phi_n\left(R_nK_n + W_nL_n^e\right)$$

Define

$$\vec{a}_n = \begin{bmatrix} a_{n,2} \\ a_{n,3} \\ \vdots \\ a_{n,G-1} \\ a_{n,G} \end{bmatrix}_{(G-1)\times 1}; \quad \vec{l} = \begin{bmatrix} l_1 \\ l_2 \\ \vdots \\ l_{G-2} \\ l_{G-1} \end{bmatrix}_{(G-1)\times 1}; \quad \vec{N}_n = \begin{bmatrix} \bar{N}_{n,1} \\ \bar{N}_{n,2} \\ \vdots \\ \bar{N}_{n,G-1} \\ \bar{N}_{n,G} \end{bmatrix}_{(G)\times 1}; \quad \Lambda_n = \begin{bmatrix} \Lambda_{n,2} \\ \Lambda_{n,3} \\ \vdots \\ \Lambda_{n,G-1} \\ \Lambda_{n,G} \end{bmatrix}_{(G-1)\times 1}$$

$$A = \begin{bmatrix} 0 & 0 & 0 & 0 & 0 & 0 \\ 1 & 0 & 0 & 0 & 0 & 0 \\ 0 & 1 & 0 & 0 & 0 & 0 \\ 0 & 0 & 1 & 0 & 0 & 0 \\ 0 & 0 & 0 & 1 & 0 & 0 \\ 0 & 0 & 0 & 0 & 1 & 0 \end{bmatrix}_{(G-1)} = \begin{bmatrix} \text{zeros}(1,G-2) & 0 \\ \text{eye}(G-2) & \text{zeros}(G-2,1) \end{bmatrix}$$

$$A' = \begin{bmatrix} 0 & 1 & 0 & 0 & 0 & 0 \\ 0 & 0 & 1 & 0 & 0 & 0 \\ 0 & 0 & 0 & 1 & 0 & 0 \\ 0 & 0 & 0 & 0 & 1 & 0 \\ 0 & 0 & 0 & 0 & 0 & 1 \end{bmatrix}_{(G-1)} \quad ; \quad I = \begin{bmatrix} 1 & 0 & 0 & 0 & 0 \\ 0 & 1 & 0 & 0 & 0 \\ 0 & 0 & 1 & 0 & 0 \\ 0 & 0 & 0 & 1 & 0 \\ 0 & 0 & 0 & 0 & 1 \end{bmatrix}_{(G-1)} = \text{eye}(G-1)$$

Equation (D.14)

$$P_{n,I}\Theta_n a_{n,g} - [\Lambda_{n,g+1}\Theta_n + G_\omega]P_{n,I}a_{n,g+1} + \Lambda_{n,g+1}G_\omega P_{n,I}a_{n,g+2} - ts_n^D[\Lambda_{n,g+1} - 1]$$

$$= W_n(1-\tau_n^L)E_n[\Lambda_{n,g+1}l_{g+1} - l_g] + ts_n^T[\Lambda_{n,g+1} - 1]; \quad \forall g \in [1, G-1]$$

can be written in matrix form as

$$\vec{a}_n = \text{LeftMatrix}^{-1} \cdot \text{RightVector}$$

where

$$\text{LeftMatrix} = [P_{n,I}\Theta_n \odot A] - [(G_\omega + \Theta_n \odot \Lambda_n)P_{n,I}] + [\Lambda_n \odot G_\omega P_{n,I} \odot A'] - [\Lambda_n - 1] \odot P_{n,I}\Theta_n \odot T$$

$$\text{RightVector} = W_n(1-\tau_n^L)E_n\left[\Lambda_n \odot A' - I\right] \times \vec{l} + [\Lambda_n - 1]ts_n^T \odot \text{ones}(G-1,1)$$

$$ts_n^D = P_{n,I}\Theta_n \sum_{g=2}^{G} \left(\frac{\bar{N}_{n,g-1}}{1+g_n} - \bar{N}_{n,g} \right) a_{n,g}$$

$$= P_{n,I}\Theta_n \odot \left\{ \bar{N}_{n,g-1}(1:G-1,1)./(1+g_n) - \bar{N}_{n,g}(2:G,1) \right\}' \times \bar{a}_n$$

$$= P_{n,I}\Theta_n \odot \left[\text{ones}(G-1,1) \times \left(\frac{\bar{N}_{n,g-1}(1:G-1,1)}{1+g_n} - \bar{N}_{n,g}(2:G,1) \right)^T \times \bar{a}_n \right]$$

$$= P_{n,I}\Theta_n \odot T \times \bar{a}_n$$

and

$$T = \text{ones}(G-1,1) \times \left(\bar{N}_{n,g-1}(1:G-1,1)./(1+g_n) - \bar{N}_{n,g}(2:G,1) \right)^T$$

C.2.II. Algorithm to compute the transition path

Algorithm 2 Open Economy Dynamic Equilibrium

1: Guess $\overline{K}^1_{t=2,\ldots,T} = \{K_1, \ldots, K_N\}^i$. The economy reaches a new steady state at $T+1$. The population dynamics reach the steady state at some time before $T+1$.

2: Get $\overline{I}^1_{t=1,\ldots,T} = \{I_1, \ldots, I_N\}^i_{t=1,\ldots,T}$, where $I^i_{n,t} = K^i_{n,t+1} - (1-\delta)K^i_{n,t}, \forall n \in \mathcal{N}$.

3: Solve the multi-sector (capital and labor as inputs with different shares across sectors) EK trade model under fixed world GDP, get $\{\pi^{ij}_n, P^j_n, I_n, R_n, C_n, W_n\}^1$.

4: Guess $\overrightarrow{tr}^{D,i,j}$, repeat the following until $\overrightarrow{tr}^{D,i,j}$ converges at some j_0, and set $\overrightarrow{tr}^{D,i}_{j_0} = \overrightarrow{tr}^{D,i,j}$:

(a) Solve $\forall G_0 \in \{1, \ldots, (G-1)\}$ Euler equations for each Country $n \in \mathcal{N}$, each beginning cohort $g_0 \in \{1, \ldots, (G-1)\}$, and begin year $t_0 \in \{1, \ldots, T\}$:

$$\{a_{n,g_0,t_0}, a_{n,g_0+G_0,t_0+G_0}, \{c_{n,g,t+g-1}\}^{g_0+G_0-1}_{g=g_0}, \{a_{n,g,t+1+g}\}^{g_0+G_0-1}_{g=g_0}\}$$

(b) For j, check:

$$\left\| \overrightarrow{tr}^{D,i,j} - \overrightarrow{tr}^{D,i,j'} \right\| < \varepsilon \cdot 1E-2$$

If it holds, return the value of $\overrightarrow{tr}^{D,i,j}$ and go to step 5; if not, update $\overrightarrow{tr}^{D,i,j+1}$ with:

$$\overrightarrow{tr}^{D,i,j+1} = \zeta' \overrightarrow{tr}^{D,i,j} + (1-\zeta')\overrightarrow{tr}^{D,i,j'}, \quad \zeta' \in (0,1)$$

Repeat from step 4.(a) with $j = j+1$ until it holds.

5: For i, calculate $\overline{K}^i_n$ for each Country $n \in \mathcal{N}$. Check $\left\| \overline{K}^i - \overline{K}^{i'} \right\| < \varepsilon$

6: **if** it holds **then**

7: Return the value of $\overline{K}^i$ and stop.

8: **else**

9: Update $\overline{K}^{i+1}$ with:

$$\overline{K}^{i+1} = \zeta \overline{K}^{i'} + (1-\zeta)\overline{K}^i, \quad \zeta \in (0,1)$$

10: Repeat from step 2 with $i = i+1$ until it holds.

11: **end if**

C.2.II.1 Detail for Step 4 :

$$\frac{c_{n,g+1,t+1}}{c_{n,g,t}} = \left[\beta \left(s_{n,g+1,t+1} \frac{\psi_{n,t+1}}{\psi_{n,t}} \frac{P_{n,I,t+1}}{P_{n,C,t+1}} \left(1 + \frac{R_{n,t+1}}{P_{n,I,t+1}} - \delta\right)\right)\right]^\sigma = \left[\beta S_{n,g+1,t+1} \Theta_{n,t+1} \frac{P_{n,IC,t+1}}{P_{n,IC,t}}\right]^\sigma$$

Define

$$S_{n,g+1,t+1} \equiv s_{n,g+1,t+1} \frac{\psi_{n,t+1}}{\psi_{n,t}}, \quad \Theta_{n,t+1} \equiv 1 + \frac{R_{n,t+1}}{P_{n,I,t+1}} - \delta = 1 + r_{n,t+1}, \quad P_{n,IC,t} \equiv \frac{P_{n,I,t}}{P_{n,C,t}}.$$

Thus

$$\frac{c_{n,g+1,t+1}}{c_{n,g,t}} = \left[\beta S_{n,g+1,t+1} \Theta_{n,t+1} \frac{P_{n,IC,t+1}}{P_{n,IC,t}}\right]^{\sigma},$$

and

$$\frac{P_{n,C,t+1} c_{n,g+1,t+1}}{P_{n,C,t} c_{n,g,t}} = \left[\beta S_{n,g+1,t+1} \Theta_{n,t+1} \frac{P_{n,C,t+1}^{1/\sigma-1} P_{n,I,t+1}}{P_{n,C,t}^{1/\sigma-1} P_{n,I,t}}\right]^{\sigma} = \left[\beta S_{n,g+1,t+1} \Theta_{n,t+1} \frac{P_{n,C\sigma I,t+1}}{P_{n,C\sigma I,t}}\right]^{\sigma}.$$

$$\frac{P_{n,C,t+1} c_{n,g+1,t+1}}{P_{n,C,t} c_{n,g,t}} = \left[\beta S_{n,g+1,t+1} \Theta_{n,t+1} P_{n,\sigma,t+1}\right]^{\sigma}.$$

Define $P_{n,C\sigma I,t} \equiv P_{n,C,t}^{1/\sigma-1} P_{n,I,t}$, $P_{n,\sigma,t+1} \equiv \dfrac{P_{n,C\sigma I,t+1}}{P_{n,C\sigma I,t}}$, $\Lambda_{n,g+1,t+1} \equiv \left[\beta S_{n,g+1,t+1} \Theta_{n,t+1} P_{n,\sigma,t+1}\right]^{-\sigma}$.

Thus

$$P_{n,C,t} c_{n,g,t} = \left[\beta S_{n,g+1,t+1} \Theta_{n,t+1} P_{n,\sigma,t+1}\right]^{-\sigma} P_{n,C,t+1} c_{n,g+1,t+1} = \Lambda_{n,g+1,t+1} P_{n,C,t+1} c_{n,g+1,t+1}.$$

$$P_{n,C,t} c_{n,g,t} = \Lambda_{n,g+1,t+1} P_{n,C,t+1} c_{n,g+1,t+1}.$$

Substitute PC into the above formula, I have

$$P_{n,I,t} \Theta_{n,t} a_{n,g,t} - P_{n,I,t} a_{n,g+!,t+1} + W_{n,t}\left(1 - \tau_{n,t}^{L}\right) E_{n,t} l_{g} + ts_{n,t}^{D} + ts_{n,t}^{T} =$$

$$\Lambda_{n,g+1,t+1}\left[P_{n,I,t+1} \Theta_{n,t+1} a_{n,g+1,t+1} - P_{n,I,t+1} a_{n,g+2,t+2} + W_{n,t+1}\left(1 - \tau_{n,t+1}^{L}\right) E_{n,t+1} l_{g+1} + ts_{n,t+1}^{D} + ts_{n,t+1}^{T}\right].$$

If the above Euler equation is solved from (g,t) to $(g+G_0-1, t+G_0-1)$, which implies G_0 unknown variables under G_0 equations, with the given value of $a_{n,g,t}$ and $a_{n,g+G_0+1,t+G_0+1}$, the first and last equation are:

$$P_{n,I,t} \Theta_{n,t} a_{n,g,t} - \left[P_{n,I,t} + \Lambda_{n,g+1,t+1} P_{n,I,t+1} \Theta_{n,t+1}\right] a_{n,g+1,t+1} + \Lambda_{n,g+1,t+1} P_{n,I,t+1} a_{n,g+2,t+2}$$

$$= \left[\Lambda_{n,g+1,t+1} W_{n,t+1}\left(1 - \tau_{n,t+1}^{L}\right) E_{n,t+1} l_{g+1} - W_{n,t}\left(1 - \tau_{n,t}^{L}\right) E_{n,t} l_{g}\right] + \left[\Lambda_{n,g+1,t+1} ts_{n,t+1}^{D} - ts_{n,t}^{D}\right]$$

$$+ \left[\Lambda_{n,g+1,t+1} ts_{n,t+1}^{T} - ts_{n,t}^{T}\right],$$

and

$$P_{n,I,t+G_0-1} \Theta_{n,t+G_0-1} a_{n,g+G_0-1,t+G_0-1} - \left[P_{n,I,t+G_0-1} + \Lambda_{n,g+G_0,t+G_0} P_{n,I,t+G_0} \Theta_{n,t+G_0}\right] a_{n,g+G_0,t+G_0}$$

$$+ \Lambda_{n,g+G_0,t+G_0} P_{n,I,t+G_0} a_{n,g+G_0+1,t+G_0+1} =$$

$$\left[\Lambda_{n,g+G_0,t+G_0} W_{n,t+G_0}\left(1 - \tau_{n,t+G_0}^{L}\right) E_{n,t+G_0} l_{g+G_0} - W_{n,t+G_0-1}\left(1 - \tau_{n,t+G_0-1}^{L}\right) E_{n,t+G_0-1} l_{g+G_0-1}\right]$$

$$+\left[\Lambda_{n,g+G_0,t+G_0} ts^D_{n,t+G_0} - ts^D_{n,t+G_0-1}\right] + \left[\Lambda_{n,g+G_0,t+G_0} ts^T_{n,t+G_0} - ts^T_{n,t+G_0-1}\right].$$

Define

$$\overrightarrow{a}_n \equiv \begin{bmatrix} a_{n,g+1,t+1} \\ a_{n,g+2,t+2} \\ \vdots \\ a_{n,g+G_0-1,t+G_0-1} \\ a_{n,g+G_0,t+G_0} \end{bmatrix}_{(G_0)\times 1} ; \overrightarrow{a}^*_{n,g,t} \equiv \begin{bmatrix} a_{n,g,t} \\ 0 \\ \vdots \\ 0 \\ 0 \end{bmatrix}_{(G_0)\times 1} ; \overrightarrow{a}^{**}_{n,g+G_0+1,t+G_0+1} \equiv \begin{bmatrix} 0 \\ 0 \\ \vdots \\ 0 \\ a_{n,g+G_0+1,t+G_0+1} \end{bmatrix}_{(G_0)\times 1} ;$$

$$A \equiv \begin{bmatrix} 0 & 0 & 0 & 0 & 0 \\ 1 & 0 & 0 & 0 & 0 \\ 0 & 1 & 0 & 0 & 0 \\ 0 & 0 & 1 & 0 & 0 \\ 0 & 0 & 0 & 1 & 0 \end{bmatrix} = [\text{zeros}(1, G_0); eyes(G_0-1) zeros(G_0-1,1)]\,; E \equiv eyes(G_0).$$

$$A' \equiv \begin{bmatrix} 0 & 1 & 0 & 0 & 0 & 0 \\ 0 & 0 & 1 & 0 & 0 & 0 \\ 0 & 0 & 0 & 1 & 0 & 0 \\ 0 & 0 & 0 & 0 & 1 & 0 \\ 0 & 0 & 0 & 0 & 0 & 1 \\ 0 & 0 & 0 & 0 & 0 & 0 \end{bmatrix} ; \quad \overrightarrow{\Theta P}_n \equiv \begin{bmatrix} \Theta_{n,t} P_{n,I,t} \\ \Theta_{n,t+1} P_{n,I,t+1} \\ \vdots \\ \Theta_{n,t+G_0-2} P_{n,I,t+G_0-2} \\ \Theta_{n,t+G_0-1} P_{n,I,t+G_0-1} \end{bmatrix}_{(G_0)\times 1} ;$$

$$\overrightarrow{\Lambda P}_n \equiv \begin{bmatrix} \Lambda_{n,g+1,t+1} P_{n,I,t+1} \\ \vdots \\ \vdots \\ \Lambda_{n,g+G_0,t+G_0} P_{n,I,t+G_0} \end{bmatrix}_{(G_0)\times 1} ;$$

$$P\Lambda\overrightarrow{\Theta P}_n \equiv \begin{bmatrix} P_{n,I,t} + \Lambda_{n,g+1,t+1} \Theta_{n,t+1} P_{n,I,t+1} \\ \vdots \\ \vdots \\ P_{n,I,t+G_0-1} + \Lambda_{n,g+G_0,t+G_0} \Theta_{n,t+G_0} P_{n,I,t+G_0} \end{bmatrix}_{(G_0)\times 1} ;$$

$$\overrightarrow{l}(g+1:g+G_0)^T \equiv \begin{bmatrix} l_{g+1} \\ l_{g+2} \\ \vdots \\ l_{g+G_0} \end{bmatrix}_{(G_0)\times 1} ; \quad \overrightarrow{l}(g:g+G_0-1)^T \equiv \begin{bmatrix} l_g \\ l_{g+2} \\ \vdots \\ l_{g+G_0-1} \end{bmatrix}_{(G_0)\times 1} ;$$

$$A\overrightarrow{a}_n+E\overrightarrow{a}^*_{n,g,t}=\begin{bmatrix} a_{n,g,t} \\ a_{n,g+1,t+1} \\ \vdots \\ a_{n,g+G_0-2,t+G_0-2} \\ a_{n,g+G_0-1,t+G_0-1} \end{bmatrix}_{(G_0)\times 1} \quad ; \quad A'\overrightarrow{a}_n+E\overrightarrow{a}^*_{n,g+G_0+1,t+G_0+1}=\begin{bmatrix} a_{n,g+2,t+2} \\ a_{n,g+3,t+3} \\ \vdots \\ a_{n,g+G_0,t+G_0} \\ a_{n,g+G_0+1,t+G_0+1} \end{bmatrix}_{(G_0)\times 1} \quad ;$$

$$\Lambda\overrightarrow{W}El_n=\begin{bmatrix} \Lambda_{n,g+1,t+1}W_{n,t+1}\left(1-\tau^L_{n,t+1}\right)E_{n,t+1}l_{g+1} \\ \vdots \\ \vdots \\ \Lambda_{n,g+G_0,t+G_0}W_{n,t+G_0}\left(1-\tau^L_{n,t+G_0}\right)E_{n,t+G_0}l_{g+G_0} \end{bmatrix}_{(G_0)\times 1} \quad ;$$

$$W\overrightarrow{E}l_n=\begin{bmatrix} W_{n,t}\left(1-\tau^L_{n,t}\right)E_{n,t}l_g \\ \vdots \\ \vdots \\ W_{n,t+G_0-1}\left(1-\tau^L_{n,t+G_0-1}\right)E_{n,t+G_0-1}l_{g+G_0-1} \end{bmatrix}_{(G_0)\times 1} \quad ;$$

$$\Lambda ts\overrightarrow{D}_n=\begin{bmatrix} \Lambda_{n,g+1,t+1}ts^D_{n,t+1}-ts^D_{n,t} \\ \vdots \\ \vdots \\ \Lambda_{n,g+G_0,t+G_0}ts^D_{n,t+G_0}-ts^D_{n,t+G_0-1} \end{bmatrix}_{(G_0)\times 1} ; \Lambda ts\overrightarrow{T}_n=\begin{bmatrix} \Lambda_{n,g+1,t+1}ts^T_{n,t+1}-ts^T_{n,t} \\ \vdots \\ \vdots \\ \Lambda_{n,g+G_0,t+G_0}ts^T_{n,t+G_0}-ts^T_{n,t+G_0-1} \end{bmatrix}_{(G_0)\times 1} \quad ;$$

Here, $ts^T_{n,t}\equiv\dfrac{D_{n,t}}{N_{n,t}}$ and $D_{n,t}=-\phi_{n,t}\left(R_{n,t}K_{n,t}+W_{n,t}L^e_{n,t}\right)+\dfrac{N_{n,t}}{\sum_N N_{n,t}\sum_{n=1}^N}\phi_{n,t}\left(R_{n,t}K_{n,t}+W_{n,t}L^e_{n,t}\right)$.

$$ts^D_{n,t}\equiv P_{n,I,t}\left(1+\frac{R_{n,t}}{P_{n,I,t}}-\delta\right)\frac{\sum_{g=2}^G\left(N_{n,g-1,t-1}-N_{n,g,t}\right)a_{n,g,t}}{N_{n,t}}$$

$$=\frac{P_{n,I,t}}{N_{n,t}}\Theta_{n,t}\left[\left(\overrightarrow{N}_{n,t-1}(1:G-1,1)-\overrightarrow{N}_{n,t}(2:G,1)\right)^T\times\overrightarrow{a}_{n,g,t}(2:G,1)\right].$$

Thus,

$$Leftside\equiv\overrightarrow{\Theta P}_n\circ\left[A\overrightarrow{a}_n+E\overrightarrow{a}^*_{n,g,t}\right]-P\Lambda\overrightarrow{\Theta P}_n\circ\overrightarrow{a}_n+\Lambda\overrightarrow{P}_n\circ\left[A'\overrightarrow{a}_n+E\overrightarrow{a}^*_{n,g+G_0+1,t+G_0+1}\right]$$

$$=\left[\overrightarrow{\Theta P}_n\circ A-P\Lambda\overrightarrow{\Theta P}_n\circ E+\Lambda\overrightarrow{P}_n\circ A'\right]\overrightarrow{a}_n+\left[\overrightarrow{\Theta P}_n\circ E\overrightarrow{a}^*_{n,g,t}+\Lambda\overrightarrow{P}_n\circ E\overrightarrow{a}^*_{n,g+G_0+1,t+G_0+1}\right],$$

$$Matrix \equiv \left[\overrightarrow{\Theta P}_n \circ A - P\Lambda\overrightarrow{\Theta P}_n \circ E + \Lambda\overrightarrow{P}_n \circ A'\right], \quad Res \equiv \left[\overrightarrow{\Theta P}_n \circ E\overrightarrow{a}^*_{n,g,t} + \Lambda\overrightarrow{P}_n \circ E\overrightarrow{a}^*_{n,g+G_0+1,t+G_0+1}\right]$$

$$Rightside \equiv \Lambda\overrightarrow{W}El_n - W\overrightarrow{E}l_n + \Lambda ts\overrightarrow{D}_n + \Lambda ts\overrightarrow{T}_n,$$

$$\overrightarrow{a_n} = Matrix^{-1}(Rightside - Res).$$

One can solve for $\overrightarrow{c_n}$ from:

$$\begin{bmatrix} P_{n,C,t} \\ P_{n,C,t+1} \\ \vdots \\ P_{n,C,t+G_0-1} \\ P_{n,C,t+G_0} \end{bmatrix}_{(G_0+1)\times 1} \begin{bmatrix} c_{n,g,t} \\ c_{n,g+1,t+1} \\ \vdots \\ c_{n,g+G_0,t+G_0} \end{bmatrix}_{(G_0+1)\times 1} = \begin{bmatrix} \Theta_{n,t}P_{n,I,t}a_{n,g,t} \\ \vdots \\ \vdots \\ \Theta_{n,t+G_0}P_{n,I,t+G_0}a_{n,g+G_0,t+G_0} \end{bmatrix}_{(G_0+1)\times 1}$$

$$- \begin{bmatrix} P_{n,I,t} \\ \vdots \\ P_{n,I,t+G_0} \end{bmatrix}_{(G_0+1)\times 1} \begin{bmatrix} a_{n,g,t+1} \\ \vdots \\ a_{n,g+G_0+1,t+G_0+1} \end{bmatrix}_{(G_0+1)\times 1} + \begin{bmatrix} W_{n,t}\left(1-\tau^L_{n,t}\right)E_{n,t}l_g \\ \vdots \\ W_{n,t+G_0}\left(1-\tau^L_{n,t+G_0}\right)E_{n,t+G_0}l_{g+G_0} \end{bmatrix}_{(G_0+1)\times 1}$$

$$+ \begin{bmatrix} ts^D_{n,t} + ts^T_{n,t} \\ \vdots \\ ts^D_{n,t+G_0} + ts^T_{n,t+G_0} \end{bmatrix}_{(G_0+1)\times 1},$$

and

$$\begin{bmatrix} i_{n,g,t} \\ i_{n,g+1,t+1} \\ \vdots \\ i_{n,g+G_0-1,t+G_0-1} \\ i_{n,g+G_0,t+G_0} \end{bmatrix}_{(G_0+1)\times 1} = \begin{bmatrix} a_{n,g+1,t+1} \\ \vdots \\ \vdots \\ a_{n,g+G_0+1,t+G_0+1} \end{bmatrix}_{(G_0+1)\times 1} - (1-\delta)\begin{bmatrix} a_{n,g,t} \\ \vdots \\ a_{n,g+G_0,t+G_0} \end{bmatrix}_{(G_0+1)\times 1}$$

$$
-\begin{bmatrix} ts^{D,1}_{n,t} \\ ts^{D,1}_{n,t+1} \\ \vdots \\ ts^{D,1}_{n,t+G_0-1} \\ ts^{D,1}_{n,t+G_0} \end{bmatrix}_{(G_0+1)\times 1} / \begin{bmatrix} P_{n,I,t} \\ P_{n,I,t+1} \\ \vdots \\ P_{n,I,t+G_0-1} \\ P_{n,I,t+G_0} \end{bmatrix}_{(G_0+1)\times 1} .
$$

Appendix D: Numerical Experiments Illustrating Model Mechanisms

In this section, through numerical experiments on both the stationary balanced growth equilibrium and the dynamic transitional equilibrium, I discuss the key mechanisms of the model.

The differences in demographic structure arise from variations in survival and fertility rates, denoted as $s_{g,t}$, the probability of surviving to age g at time t, given that one was alive at age $g-1$, and $f_{g,t}$, the number of newborns from each age g cohort at time t. Figure D.1 shows the age-varying survival rate and fertility rate for two steady states, one with a high average level and one with a low average level. The main difference in the left-side figure between the two survival rate series is that after age 35, the red line has a higher survival rate on average for each age above 35. The implied average lifespan for the red line is thus longer than for the blue. The main difference in the right-side figure is that, on average, the red line shows a higher level of average fertility rate.

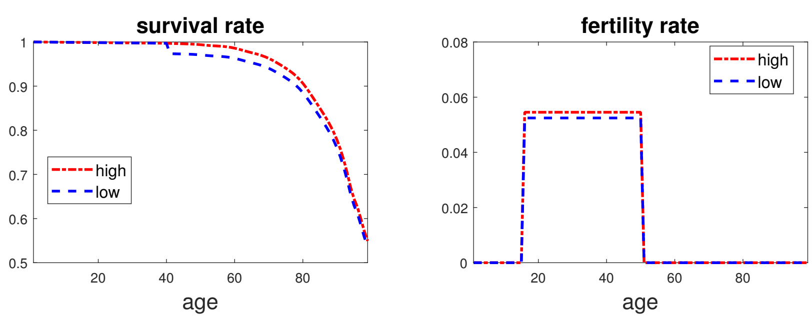

Figure D.1
Fertility rate and survival rate

$$
\frac{\lambda_{t+1}-\lambda_t}{\lambda_t} = \Gamma\left(1-\rho\right)\alpha_t\left(\lambda_t\right)^{\rho-1}; \qquad \alpha_t \equiv \left(\sum_g \eta_g N_{g,t}\right)^{\varphi} \tag{D.1}
$$

To show how demographic structure affects knowledge stocks over time, I present a simple application. Assuming that the economy is on a balanced growth path in the initial period and that only working-age people contribute to new idea generation, I have:

$$
\eta_g = c > 0 \quad \text{if} \quad g \in (16,65), \quad \text{and} \quad \eta_g = 0 \quad \text{if} \quad g \notin (16,65).
$$

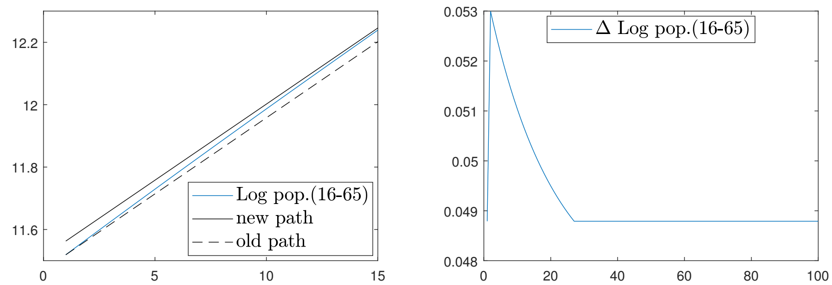

Figure D.2
Population dynamics: from low survival rate to high

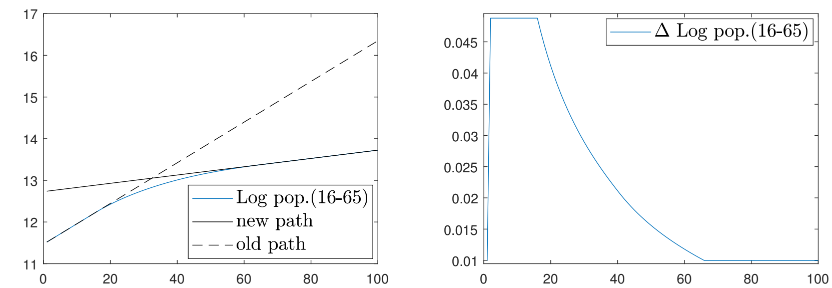

Figure D.3
Population dynamics: from high fertility to low

D.0.I. Demographics and knowledge stocks

I conduct two counterfactual experiments to show how productivity responds to demographic shocks. Figure D.2 and Figure D.3 illustrate the effects of two types of shocks.

Figure D.2 shows that when Country 1 transitions from a low survival rate to a high survival rate, all else equal. The working-age population initially increases, leading to a rise in the knowledge stock. As the growth of the working-age population slows, the growth of the knowledge stock also decelerates, eventually matching the initial growth rate (Figure D.4).

Figure D.3 shows the effect of transitioning from a high fertility rate to a low fertility rate in Country 1. All else equal, the growth of both the total population and the working-age population slows, eventually stabilizing at a lower level compared to the previous growth path, with a growth rate that remains lower than before. As the working-age population growth slows, the growth of the knowledge stock also decelerates. Once the working-age population growth rate stabilizes at a lower level, the growth of the knowledge stock will stabilize at this lower rate (Figure D.5).

Implications

An increase in the level of the working-age population leads to a higher level of knowledge stock. On the balanced growth path, higher population growth implies higher knowledge

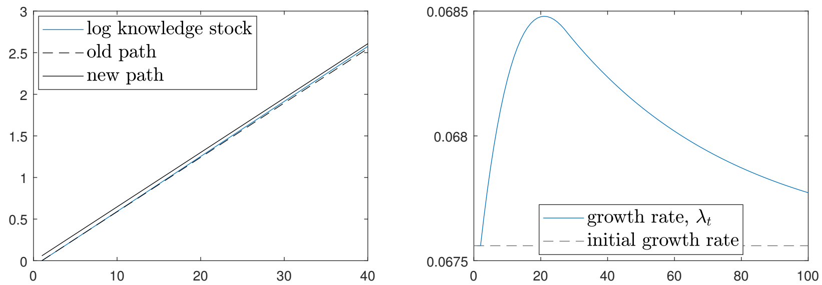

Figure D.4
Knowledge stock dynamics: from low survival rate to high

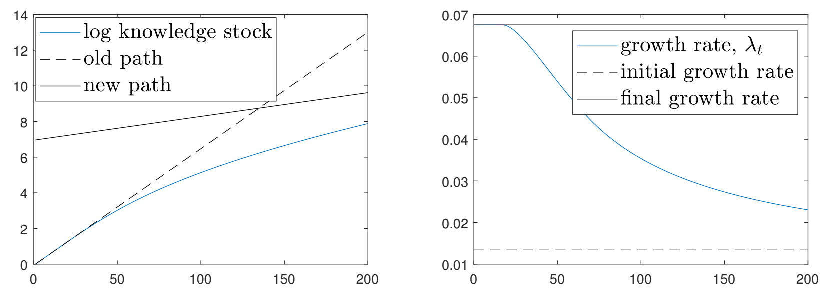

Figure D.5
Knowledge stock dynamics: from high fertility to low

stock growth.

D.0.II. Demographics and capital stocks

Besides the effects on knowledge stocks, in this paragraph, I further explore the effects of demographics on capital stocks. Specifically, I first compare balanced growth equilibria with different structures, then I show how capital and other variables change over time during the transition process from one balanced growth equilibrium to another.

Consider a 2x2 (two-country, two-sector) economy, where Sector 1 is labor-intensive and Sector 2 is capital-intensive. Table D.1 presents the stationary balanced equilibrium under various conditions. The four columns are derived from a closed economy model. Columns (1S) to (3S) depict symmetric countries, while the countries in (1A) are asymmetric. Although the model operates under a closed economy framework, the symmetry or asymmetry does not significantly affect the results. This distinction becomes relevant when analyzing the effects of trade liberalization, as the closed economy counterparts serve as a control group for evaluating trade impacts.

Comparing columns ($2S$) and ($1S$), a higher survival rate allows individuals to live longer, which in turn enhances their ability to save. This increase in savings contributes to a larger supply of capital, resulting in a higher capital per efficient person. Meanwhile, when we compare column ($3S$) with column ($2S$), a lower fertility rate leads to a slowdown in

TABLE D.1

Stationary balance growth equilibrium comparison. Close economy

	(1S)	(2S)	(3S)	(1A)	
Country	sym.	sym.	sym.	cty1	cty2
Survival rate	low	high	high	high	low
Fertility rate	high	high	low	high	high
Average lifespan	60.1	70.8	70.8	70.8	60.1
Population growth	1.050	1.050	1.010	1.050	1.050
Implied TFP growth	0.025	0.025	1.003	1.025	1.025
Working age share	0.44	0.46	0.72	0.46	0.44
Trade cost	Autarky	Autarky	Autarky	Autarky	Autarky
Capital share of VA	0.5000	0.5000	0.5000	0.5000	0.5000
Per efficient person					
Capital stock	0.007	0.009	0.022	0.009	0.007
Output	0.0026	0.0029	0.0054	0.0029	0.0026
Consumption	0.0016	0.0017	0.0038	0.0017	0.0016
Investment	0.0010	0.0012	0.0016	0.0012	0.0010
Capital - efficient labor ratio	0.016	0.019	0.030	0.019	0.016
Price ratio					
Real wage rate	0.003	0.003	0.004	0.003	0.003
Real rental rate	0.179	0.165	0.125	0.165	0.179

population growth, which also implies a deceleration in productivity growth. Consequently, less capital is distributed among efficient individuals, thereby leading to a higher capital per efficient person. Finally, the capital-labor ratio reflects a relative abundance of capital compared to labor, highlighting the significant effects of these demographic changes on the economy.

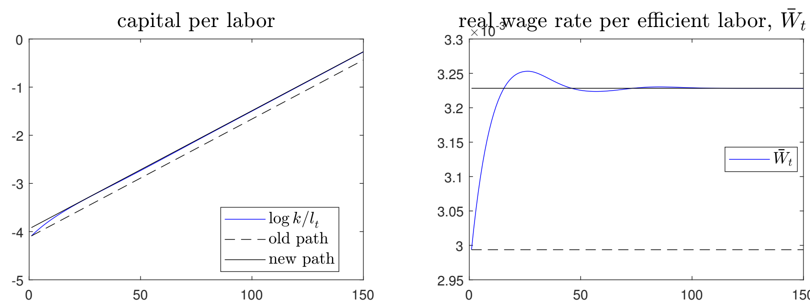

Figure D.6

living longer. Close economy

Figure D.6 illustrates how capital and other variables change over time following a positive shock to the survival rate (Figure D.7 for more details) . Basically, a higher survival rate stimulates capital accumulation and elevates the balanced growth path. In the short run, as the population of Country 1 lives longer, savings increase, resulting in higher capital per person until it reaches a new growth path.

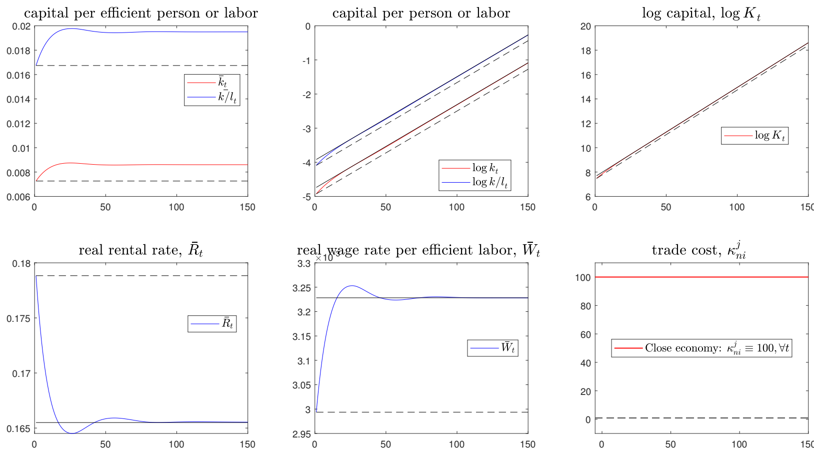

Figure D.7
LIVING LONGER. CLOSE ECONOMY

The first figure in Figure D.7 depicts both capital per labor and capital per person. The difference between these two indices reflects changes in the working-age share. The trends for capital per labor and capital per person are driven by the growth rate of the knowledge stock: the initial increase in the working-age population leads to a corresponding rise in the knowledge stock. However, as the growth of the working-age population slows, the growth of the knowledge stock also decelerates, eventually aligning with the initial growth rate.

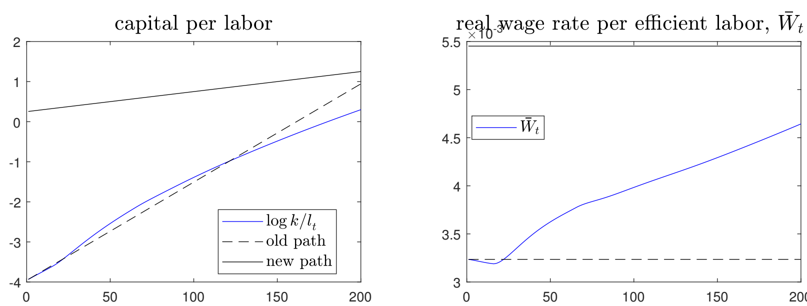

Figure D.8
POPULATION GROWTH SLOWS DOWN. CLOSE ECONOMY

Figure D.8 illustrates how capital and other variables change over time following a negative shock to the fertility rate (Figure D.9 for more details). In the short run, as the population growth rate slows down, this can be beneficial, resulting in a higher level of capital per person and capital per labor due to a reduced young population. However, in the long run, this trend is harmful, as it leads to a slowdown in productivity growth.

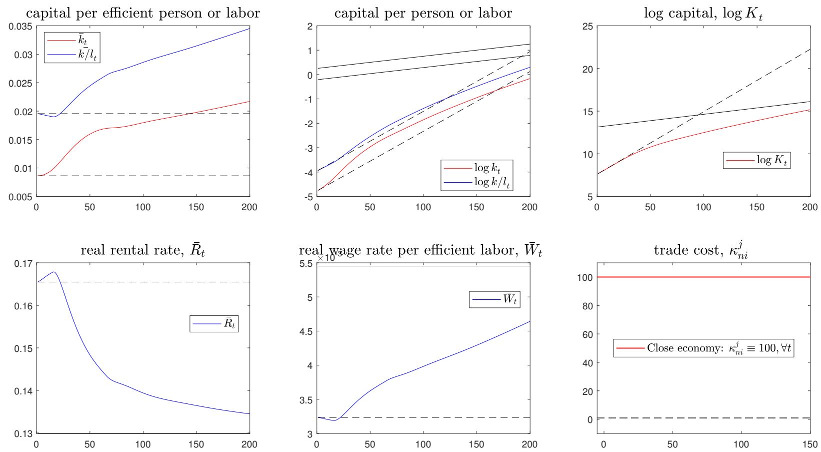

Figure D.9
Population growth slows down. Close economy

Implications

A higher survival rate stimulates capital accumulation, elevating the balanced growth path. The effects of a fertility rate shock are twofold: in the short run, a lower population growth rate raises capital per person above the previous growth path due to a reduced young population. However, in the long run, this benefit is counterbalanced by a slowdown in productivity growth, ultimately resulting in capital per person falling below the old growth path.

D.0.III. Demographics and trade

In this section, I explore the interactive effects of demographics and trade liberalization. Specifically, I first compare balanced growth equilibrium under different structural conditions, both with and without free trade. Then, I analyze how capital and other variables evolve over time during the transition process in both scenarios.

Table D.2 presents a comparison between stationary balanced growth equilibrium under free trade and autarky (no trade) conditions. The table shows different scenarios represented by columns (1S), (2S), (3S), and (1A), where "sym." indicates symmetrical countries and "cty1" and "cty2" represent two asymmetrical countries. The rows below the "Free Trade vs. Autarky (=1)" line show various economic indicators as ratios of their values under trade to those under autarky. For instance, the capital stock, output, consumption, and investment per efficient person are all equal to 2.83 in the symmetrical trade scenarios, indicating that free trade has a stimulating effect on capital accumulation across these cases. Moreover, real wage rates and real rental rates also adjust under trade conditions, reflecting shifts in productivity and capital distribution.

For the asymmetrical scenario (1A), the table indicates that "cty1" has a higher survival

TABLE D.2

STATIONARY BALANCE GROWTH EQUILIBRIUM COMPARISON. FREE TRADE V.S. CLOSE ECONOMY

	(1S)	(2S)	(3S)	(1A)	
Country	sym.	sym.	sym.	cty1	cty2
Survival rate	low	high	high	high	low
Fertility rate	high	high	low	high	high
Average lifespan	60.1	70.8	70.8	70.8	60.1
Population growth	1.050	1.050	1.010	1.050	1.050
Implied TFP growth	0.025	0.025	1.003	1.025	1.025
Working age share	0.44	0.46	0.72	0.46	0.44
Free trade v.s. Autarky(=1)					
Capital share of VA	1.000	1.000	1.000	1.002	0.998
Per efficient person					
Capital stock	2.83	2.83	2.83	2.75	2.90
Output	2.83	2.83	2.83	2.74	2.93
Consumption	2.83	2.83	2.83	2.72	2.94
Investment	2.83	2.83	2.83	2.75	2.90
Capital - efffcient labor ratio	2.83	2.83	2.83	2.75	2.90
Price ratio					
Real wage rate	2.83	2.83	2.83	2.71	2.95
Real rental rate	1.000	1.000	1.000	1.001	0.999

rate, leading to higher capital stock and investment levels compared to "cty2." This difference implies that "cty1" has a comparative advantage in producing capital-intensive goods. Consequently, the capital share of value added (VA) is higher in "cty1," indicating better allocation efficiency due to trade. Across all columns (1S, 2S, 3S, 1A), the larger supply of capital under free trade is evident, resulting from trade's selection effect. Trade encourages higher productivity and lowers prices, which in turn stimulates capital accumulation and enhances income. This improved capital accumulation, driven by trade, enables countries to reach higher levels of income.

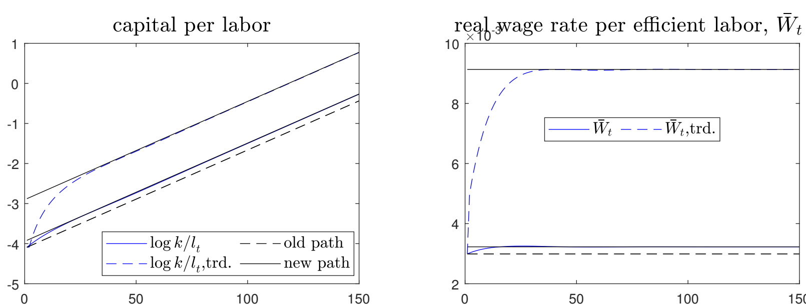

FIGURE D.10

LIVING LONGER. SYMMETRIC OPEN ECONOMY V.S. CLOSE

As depicted in Figure D.10, the economy initially operates under a closed economy setup, but from period 2 onwards, trade costs are reduced to zero, indicating the onset of free trade

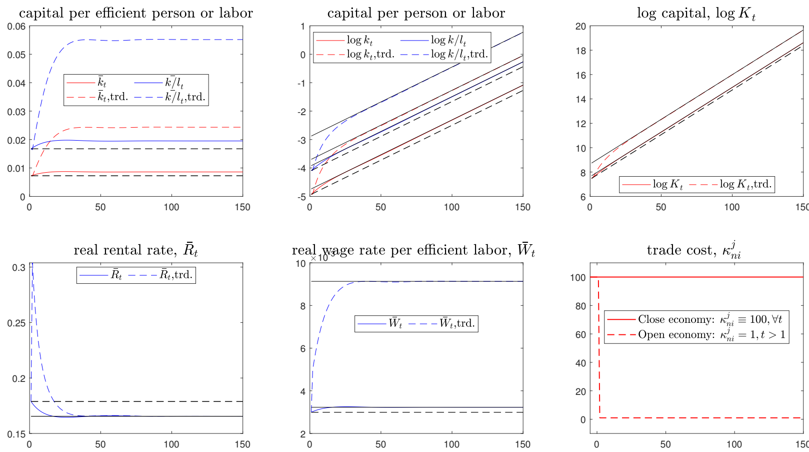

Figure D.11

living longer. Symmetric Open economy v.s. Close

(Figure D.11 for more details).

When a positive shock to the survival rate occurs, it results in higher life expectancy, which increases the incentive for saving and investing, leading to an accumulation of capital. Both in closed and open economies, this higher survival rate elevates the balanced growth path.

In addition, free trade amplifies these effects by reallocating resources more efficiently and stimulating higher productivity from selection effects, thereby boosting capital accumulation even further.

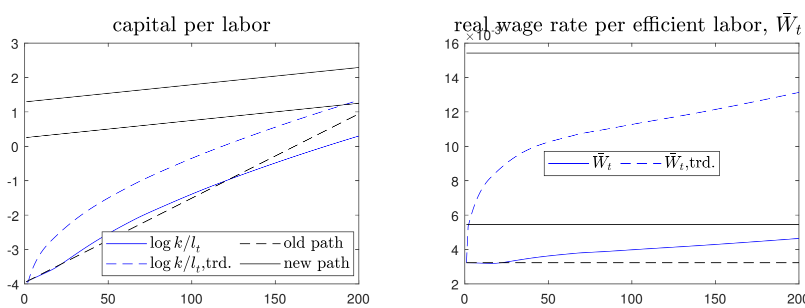

Figure D.12

Population growth slows down. Symmetric Open economy v.s. Close

In Figure D.12, the economy undergoes a negative shock to the fertility rate. Initially, the reduced population growth due to lower fertility leads to an increase in capital per person and capital per labor, enhancing productivity in the short run. However, over time, as the young population declines, there is a risk of lower labor force growth, which can ultimately harm productivity and economic growth (Figure D.13 for more details).

Trade liberalization mitigates this long-term downside by prolonging the period in which

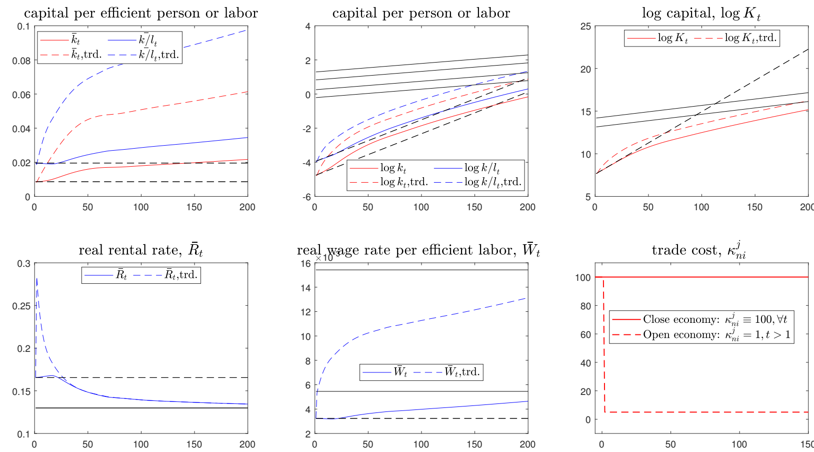

Figure D.13

Population growth slows down. Symmetric Open economy v.s. Close

capital per person remains higher than in the closed economy scenario, thereby extending the period of economic benefits. Free trade, by selection effects and enhancing resource allocation, allows the economy to sustain a higher level of capital per person for a longer duration.

Implications

A higher survival rate stimulates capital accumulation, elevating the balanced growth path. Free trade amplifies these effects by selection effects and enhancing resource allocation.

The effects of a fertility rate shock are beneficial in the short run, but adverse in the long run. Trade liberalization mitigates this long-term downside by prolonging the period in which capital per person remains higher than in the closed economy scenario, thereby extending the period of economic benefits.

Summary

A higher survival rate leads to greater knowledge stock and capital stock accumulation, raising the balanced growth path by enhancing both productivity and capital. Free trade induce specialization, which encourages higher productivity and lowers prices, ultimately leading to even greater capital accumulation.

Similarly, a lower fertility rate impacts both knowledge and capital stocks. In the short run, a reduced young population raises capital per person, temporarily boosting economic output. However, over time, this benefit is offset by slower productivity growth due to the demographic shift, ultimately causing capital per person to fall below the previous growth path. Trade liberalization can mitigate this long-term drawback by maintaining capital per person above the old growth path for a longer period, which extends the overall economic benefits in comparison to a closed economy scenario.

Appendix E: Calibration details

E.1. Selection of Countries and Sectors for Calibration

TABLE E.1
Country Groups

couty	countrycode	country_nam	couty	countrycode	country_nam
1	AUS	Australia	14	IND	India
2	AUT	Austria	15	IRL	Ireland
3	BEL	Belgium	16	ITA	Italy
4	BRA	Brazil	17	JPN	Japan
5	CAN	Canada	18	KOR	Korea, Republic of
6	CHN	China	19	MEX	Mexico
7	DEU	Germany	20	NLD	Netherlands
8	DNK	Denmark	21	PRT	Portugal
9	ESP	Spain	22	SWE	Sweden
10	FIN	Finland	23	TWN	Taiwan
11	FRA	France	24	USA	United States of America
12	GBR	United Kingdom	25	ROW	Rest of the World
13	GRC	Greece			

TABLE E.2
Sector classifications

#1.	5 Sector Classification	Index 1	Index 2	#2.	Sector Description
1	Agriculture, Mining and Quarrying	0.76	0.87	1	Agriculture, Hunting, Forestry and Fishing
1	Agriculture, Mining and Quarrying	0.40	0.34	2	Mining and Quarrying
2	Manufacture-labor intensive	0.59	0.72	3	Food, Beverages and Tobacco
2	Manufacture-labor intensive	0.64	0.72	4	Textiles, Textile, Leather and Footwear
2	Manufacture-labor intensive	0.63	0.78	5	Wood and Products of Wood and Cork
2	Manufacture-labor intensive	0.60	0.68	6	Pulp, Paper, Paper, Printing and Publishing
3	**Manufacture-capital intensive**	**0.47**	**0.44**	7	**Coke, Refined Petroleum and Nuclear Fuel**
3	**Manufacture-capital intensive**	**0.44**	**0.41**	8	**Chemicals and Chemical Products**
2	Manufacture-labor intensive	0.56	0.60	9	Rubber and Plastics
2	Manufacture-labor intensive	0.52	0.52	10	Other NonMetallic Mineral
2	Manufacture-labor intensive	0.51	0.51	11	Basic Metals and Fabricated Metal
2	Manufacture-labor intensive	0.57	0.62	12	Machinery, Nec
3	**Manufacture-capital intensive**	**0.49**	**0.44**	13	**Electrical and Optical Equipment**
2	Manufacture-labor intensive	0.55	0.56	14	Transport Equipment
2	Manufacture-labor intensive	0.66	0.81	15	Manufacturing, Nec; Recycling
3	**Manufacture-capital intensive**	**0.41**	**0.33**	16	**Electricity, Gas and Water Supply**
4	Services-labor intensive	0.72	0.93	17	Construction
4	Services-labor intensive	0.61	0.95	18	Wholesale and Retail Trade
4	Services-labor intensive	0.76	0.91	19	Hotels and Restaurants
4	Services-labor intensive	0.68	0.89	20	Transport and Storage
5	**Services-capital intensive**	**0.42**	**0.50**	21	**Post and Telecommunications**
5	**Services-capital intensive**	**0.50**	**0.51**	**22**	**Financial Intermediation**
5	**Services-capital intensive**	**0.44**	**0.40**	**23**	**Real Estate, Renting and Business Activities**
4	Services-labor intensive	0.75	0.86	24	Community Social and Personal Services

E.2. Details

For forward-looking households, it is necessary to define the time-varying processes that extend beyond the sample period of 1970–2020. The extra 80 years (2020-2100) is intentionally designed to build solid expectations for individuals born in 2020, which is the last year of interest. Thus, the model is calibrated and solved from the assumed initial steady state in 1970 to the final steady state in 2100. From 1970 to 2100, I calibrate time-varying productivity and trade costs using data on trade flow, input-output tables, capital stock, demographic variables, and sectoral prices. Data used in the calibration from 1970-2020 are historical data, while data or shocks used in the calibration from 2021-2200 are based on projections and model imputes.

For the initial steady state, the population growth rate, real wage growth rate and demographic distribution is calculated as the average value across both years from 1965–1975 and regions. Since demographic variables change slowly over time, I assume that each country is in a steady state characterized by these calculated average demographic distributions and an average constant growth rate. With these calculated average growth rates for real wages and population, plus the calibrated productivity levels in 1970, I can, on the one hand, calibrate the parameters $\eta_g, g \in [16, 65]$ in the demographic structure and knowledge stocks equation[7]. On the other hand, I calculate the model-implied saving distributions. In the steady state, the saving wedge $\psi_1^{c,\star}$ governs the saving tendency and determines both the steady-state capital stock and saving distribution, which I adjust to ensure that the model-generated capital stock matches the actual data, as I will show in the following paragraph.

For final steady state and the period after 2100, I assume that each region will maintain both its total population and population distribution, which implies that demographic parameters (fertility and survival rates) stabilize by 2100. The new steady state implies zero population growth, which also suggests a zero productivity growth rate. However, after 2100, the productivity growth rate is still approaching zero but has not yet reached it. Therefore, I calculate an average growth rate as an approximation. Specifically, given the calibrated productivity values for 2100, I impute the productivity levels for each region over the next 85 years. Then, I calculate the average productivity growth rate between 2100 and 2185. I take this average growth rate as an approximation for the growth rate on the balanced growth path. The results yield a steady-state saving distribution across different ages. These variables act as terminal conditions for the model and are key to solving the transition dynamics between the two steady states. While the assumed approximate steady state in 2100 is not a true steady state, it is sufficiently far from 2020, which is the last period of interest, so it exerts minimal influence on the period of interest.

7. For calibration details for the knowledge stock process, please refer to Appendix E.

During the period 2020–2100, data such as trade flow, input-output tables, and capital stock are not directly observable. However, I can impute these data using appropriate estimations for productivity and demographic variables. The demographic variables are obtained from UN imputations. Based on the demographic data, I can impute time-varying total factor productivity (TFP) through the demographic-knowledge stock link. I also maintain trade costs at 2020 levels for the entire period from 2020 to 2100. By solving the CP model year by year with the imputed investment rate, I can generate time series data for trade flows, sectoral prices, and other key variables[8].

E.3. Data

E.3.I. Data sources

TABLE E.3
STEADY-STATE CONDITIONS

Variable description	Model counterpart	Data source (1971–2020)	Data source (2021–2100)
Age distribution	$\tilde{N}_{n,g,t}$	UN	UN, Imputed
Population	$N_{n,t}$	PWT	UN, Imputed
Employment	$L_{n,t}$	PWT	Imputed
Human capital index	$E_{n,t}$	PWT	Imputed
Value added	$W_{n,t}L_{n,t}E_{n,t} + R_{n,t}K_{n,t}$	WIOD & Long IO Table	Imputed
Gross output*	$P^j_{n,t}y_{n,t}$	WIOD & Long IO Table	Imputed
Gross expenditure*	$P^j_{n,t}Q^j_{n,t}$	WIOD & Long IO Table	Imputed
Trade flow*	$P^j_{n,t}Q^j_{n,t}T_{n,i,t}$	WIOD & Long IO Table	Imputed
Intermediate prices**	$P^j_{n,t}$	WIOD & Long IO Table	Imputed
Consumption***	$C_{n,t}$	WIOD & Long IO Table	Imputed
Investment***	$I_{n,t}$	WIOD & Long IO Table	Imputed
Initial capital stock***	$K_{n,t0}$	PWT	N/A

Notes: * Values are measured in current prices using market exchange rates. ** Prices are measured using PPP exchange rates. *** Quantities are measured as values deflated by prices. The sources of these data are Timmer et al. (2015); Feenstra, Inklaar and Timmer (2015); United Nations and Social Affairs (2024); Woltjer, Ggouma and Timmer (2021).

E.3.II. Constructing realized data from 1970-2020

Capital stock The initial capital stock is sourced directly from the Penn World Table 10.01 Feenstra, Inklaar and Timmer (2015), which provides "Capital stock at current PPPs (in mil. 2017US$)." This data allows me to align the initial aggregate capital stocks, $K_{n,t0}$, with my model.

8. The investment rate is imputed by estimating the relationship between the investment rate, a country-fixed effect, the lagged investment rate, and the contemporaneous demographic index for the years 1965–2020. Check Appendix E for details.

Data on aggregate and sectoral investment values ($PI_{n,t}, PI^j_{n,t}$) is taken from the World Input-Output Database Timmer et al. (2015); Woltjer, Ggouma and Timmer (2021). The Penn World Table 10.01 also offers "Capital stock at constant 2017 national prices (in mil. 2017US$)," which is used to impute the initial investment price level for the first period:

$$I^{PWT}_{n,t1} = K^{PWT}_{n,t2} - (1-\delta)K^{PWT}_{n,t1},$$

and

$$P^{Implied}_{I,n,t1} = \frac{PI^{IO}_{n,t1}}{I^{PWT}_{n,I,t1}}, \quad \text{where} \quad P_{I,n,t} \equiv \prod_{j=1}^{J} \left[\frac{P^j_{n,t}}{\alpha^j_{I,n}} \right]^{\alpha^j_{I,n}}.$$

The sectoral intermediate prices for the base country are derived from the World Input-Output Database Social Economic Account, while for other regions, these prices are imputed using a gravity equation and model-implied relations. These sectoral intermediate prices ($P^{IO,j}_{n,t}$) are then used to compute the implied prices for investment ($P^{IO}_{I,n,t}$) and consumption ($P^{IO}_{C,n,t}$).

To correct the level of sectoral intermediate prices which is implied in the PWT capital stock variable, I apply the following scaling:

$$P^{scaled,j}_{n,t1} = P^{IO,j}_{n,t1} \frac{P^{Implied}_{I,n,t1}}{P^{IO}_{I,n,t1}}, \quad t = t_1$$

and for subsequent periods,

$$P^{scaled,j}_{n,tx} = P^{scaled,j}_{n,t1} \frac{P^{IO,j}_{n,tx}}{P^{IO,j}_{n,t1}}, \quad t_x > t_1.$$

These scaled sectoral prices, $P^{scaled,j}_{n,t}$, allow me to calculate the quantity of investment $I_{n,t}$ and capital stock $K_{n,t}$ over time.

Consumption or investment Final demand part of IO table includes: Final consumption expenditure by households, Final consumption expenditure by non-profit organisations serving households (NPISH), Final consumption expenditure by government, Gross fixed capital formation, Changes in inventories and valuables. I set

$$\text{Consumption} = \text{Government consumption} + \text{Household Consumption}$$

$$\text{Investment} = \text{Final demand} - \text{consumption}$$

E.3.III. Constructing realized data from 2020-2200

Investment Define investment rate as $sr_{n,t} = \frac{P_{n,I,t}I_{n,t}}{IN_{n,t}}$ where $IN_{n,t} \equiv R_{n,t}K_{n,t}+W_{n,t}E_{n,t}L_{n,t}+D_{n,t}$. I estimate the relationship between the investment rate against a country-fixed effect, the lagged investment rate, the contemporaneous and lagged demographic index, and the contemporaneous and lagged real GDP per capita for the years 1965-2020.

$$\log\left(\frac{sr_{n,t}}{1-sr_{n,t}}\right) = \alpha_0 + \alpha_1 \log\left(\frac{sr_{n,t-1}}{1-sr_{n,t-1}}\right) + \alpha_2 Young_{n,t} + \alpha_3 Old_{n,t} + f_n + \epsilon_{n,t}$$

Using $\log\left(\frac{sr}{1-sr}\right)$ ensures that the imputed values of sr lie within the interval (0, 1).

TABLE E.4
SAVING RATE REGRESSION

	(1)	(2)	(3)
VARIABLES	SR	SR	SR
L1.SR		0.89***	
		(32.74)	
L5.SR	0.43***		
	(8.04)		
Young share	-1.06***	-0.19	-2.80***
	(-3.62)	(-1.34)	(-10.75)
Old share	-2.40***	-0.45*	-5.97***
	(-4.37)	(-1.66)	(-12.36)
Constant	-0.22**	-0.04	0.04
	(-2.24)	(-0.84)	(0.36)
Observations	255	275	280
R-squared	0.891	0.968	0.836
Region FE	YES	YES	YES

E.4. Calibrate Knowledge stock process

The process of knowledge stock is formulated as:

$$\frac{\lambda_{(n,t+1)} - \lambda_{(n,t)}}{\lambda_{(n,t)}} = \left(\lambda_{(n,t)}\right)^{\rho-1}\left[\sum_g \eta_g N_{(n,g,t)}\right]^{\varphi} \Gamma(1-\rho)$$

Here, following Buera and Oberfield (2020), I set $\rho = 0.7$ and calibrate φ.
On the balanced growth path, the knowledge stock formula can be written as:

$$1 + g_{\lambda,t+1} = 1 + g_\lambda = \left(\lambda_{(n,t)}\right)^{\rho-1} N_{n,t}^{\varphi}\left[\sum_g \eta_g \bar{N}_{(n,g)}\right]^{\varphi} \Gamma(1-\rho)$$

Thus, on the balanced growth path (BLG), population and knowledge stock must grow at a constant rate, with the relation:

$$(1 + g_\lambda)^{1-\rho} = (1 + g_n)^\varphi$$

where $1+g_n$ can be calculated from the population growth rate in 1970, and then averaged across regions. $1 + g_\lambda$ can be backed out from the real wage growth rate with the relation:

$$1 + g_{\text{real wage}} = (1 + g_\lambda)^{1/\theta\beta\gamma}$$

I then take the average across regions. Thus,

$$\varphi = \frac{(1-\rho)\log(1+g_\lambda)}{\log(1+g_n)}$$

To calibrate η_g, I assume that all working-age people have the same $\eta_g > 0$. In 1970, the world economy is assumed to be on the balanced growth path, which implies

$$1 + g_{\lambda,1970} = (\lambda_{n,1970})^{\rho-1} \left[\sum_{g\in[16,65]} \eta_g N_{n,g,1970} \right]^\varphi \Gamma(1-\rho)$$

Thus,

$$\eta_g = \frac{1 + g_{\lambda,1970}}{(\lambda_{n,1970})^{\rho-1} \left(N_{n,g\in[16,65],1970}\right)^\varphi \Gamma(1-\rho)}.$$

E.5. Calibrate saving (or investment) wedges

The model suggests that higher saving wedges, $\psi_{n,t}$, indicate a stronger incentive to save for period t. Since savings provide the supply of investment, this leads to a higher capital stock in that period. Therefore, I use the aggregate capital stock, $K_{n,t}$, as targets to calibrate the evolution of saving wedges, $\psi_{n,t}$, over time.

E.5.I. Calibrate saving (or investment) wedges at steady state, ϕ_n

At the initial year, I assume the economy is in a steady state. I thus introduce the saving wedges, ψ_n, which serve as parameters to align the model's aggregate capital stock with the observed data. Mathematically, these parameter represent wedges to match the steady state capital stock, while intuitively, they capture the degree to which individuals discount next period's consumption. Even in the steady state, this variable can be included as it reflects the discount rate applied to next periods (or more precisely, to next ages), influencing saving behavior and ultimately affecting the capital stock at steady state.

Algorithm 3 Calibrate saving wedges, ψ_n, at Steady State

1: Guess a vector of saving wedges $\tilde{\psi}^i = \{\psi_1, ..., \psi_N\}^i$.

2: Given $\{P^j_{n,t}, P_{n,I,t}, P_{n,C,t}, R_{n,t}, W_{n,t}, I_{n,t}, K_{n,t}\}$ at $t = t_0$, solve $(G-1)$ Euler equations for each Country n, as described in Algorithm 3, to get a vector of capital stocks

$$\{a^1_{n,1}, a^1_{n,G+1} = 0, \{a^1_{n,g+1}\}^{G-1}_{g=1}\}.$$

3: Calculate K'_n as

$$K'_n = \sum_{g=2}^{G} \frac{N_{n,g-1} a^1_{n,g}}{1+g_n} \quad \text{for each Country } n.$$

4: Check error term, if $\left\|\tilde{K}^{data} - \tilde{K}^i\right\| < \epsilon$, stop. Else, go to next Step.

5: Go back to step 2 with updated new guess $\tilde{\psi}^{i+1}$:

$$\tilde{\psi}^{i+1} = \tilde{\psi}^i + \zeta \frac{\tilde{K}^i - \tilde{K}^{data}}{\tilde{K}^{data}} \quad \text{where } \zeta \in (0,1).$$

E.5.II. Calibrate saving wedges during transition dynamics

Algorithm 4 Calibrate saving wedges, $\psi_{n,t}$, during transition dynamics

1: Guess a vector of capital stocks $\tilde{\psi}^i_t = \{\psi_{1,t}, ..., \psi_{N,t}\}^i$, for $t = 2, \cdots, T+1$. $\tilde{\psi}_{t=1} = \tilde{\psi}_{t=1}$ is constant.

2: Given $\{P^j_{n,t}, P_{n,I,t}, P_{n,C,t}, R_{n,t}, W_{n,t}, I_{n,t}, K_{n,t}\}^1$ for $\forall t \in [1, T+1], n \in [1, ..., N]$, as described in *Algorithm 4*, solve $\forall G_0 \in \{1, ..., (G-1)\}$ Euler equations for each Country $n \in \mathcal{N}$, each begin cohort $g_0 \in \{1, ..., (G-1)\}$, and begin year $t_0 \in \{1, ..., T\}$:

$$a_{n,g_0,t_0}, a_{n,g_0+G_0,t_0+G_0}, \{c_{n,g,t+g-1}\}^{g_0+G_0-1}_{g=g_0}, \{a_{n,g,t+1+g}\}^{g_0+G_0-1}_{g=g_0}$$

and $\overrightarrow{tr}^{D^i}$.

3: Calculate $K'^i_{n,t} = \sum_{g=2}^{G} \frac{N_{n,g-1}}{1+g_n} a^1_{n,g}$ for each Country n and $t = 2, \cdots, T+1$.

Check error term, if $\left\|\tilde{K}^{data}_{t=2,\cdots,T+1} - \tilde{K}^i_{t=2,\cdots,T+1}\right\| < \epsilon$, stop. Else, go to next step.

4: Go back to step 2 with updated new guess $\tilde{\psi}^{i+1}_{t=2,\cdots,T+1}$:

$$\tilde{\psi}^{i+1}_{t=2,\cdots,T+1} = \zeta \tilde{\psi}^i_{t=2,\cdots,T+1} + \zeta \frac{\tilde{K}^i_{t=2,\cdots,T+1} - \tilde{K}^{data}_{t=2,\cdots,T+1}}{\tilde{K}^{data}_{t=2,\cdots,T+1}} \quad \text{where } \zeta \in (0,1).$$

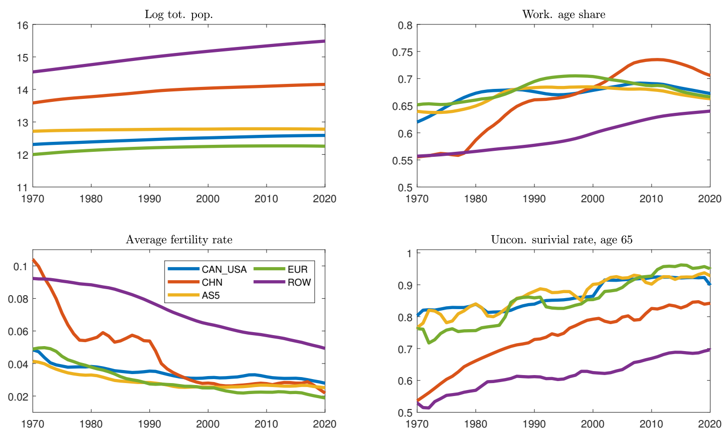

Figure E.1
Demographics

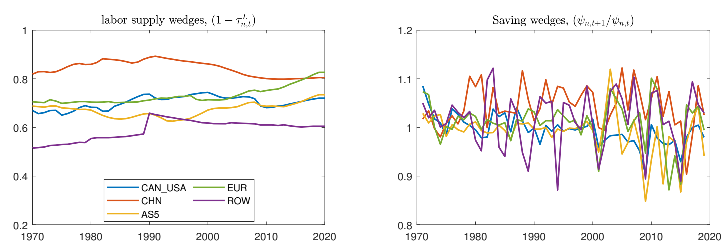

Figure E.2
Labor supply wedges and saving (or investment) wedges

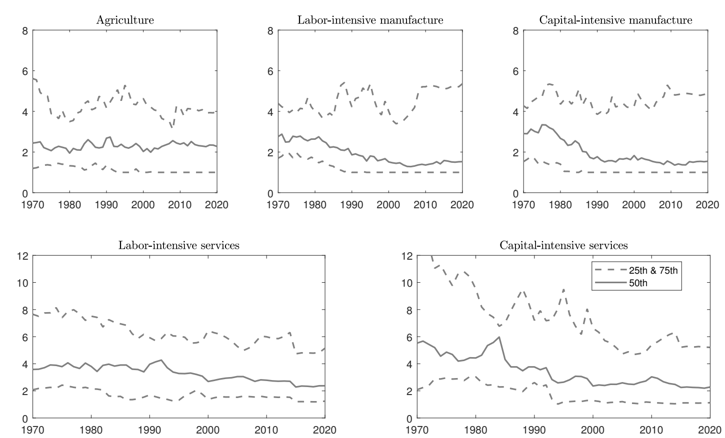

Figure E.3
Trade costs

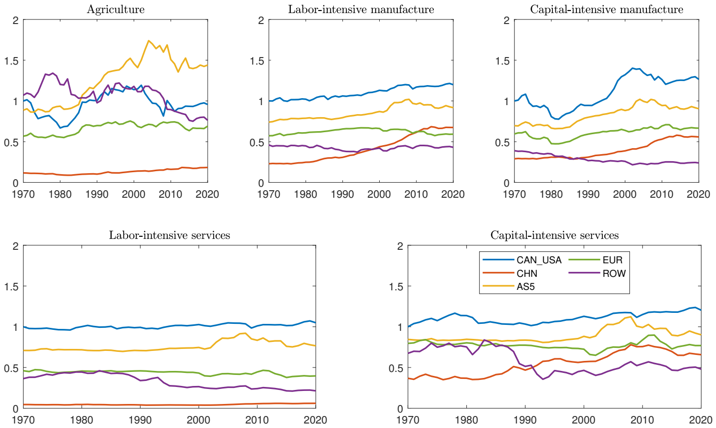

Figure E.4
Knowledge stocks

E.6. Details of calibrated shocks

Appendix F: Counterfactual analysis

F.1. Demographics, economic growth, and trade patterns change

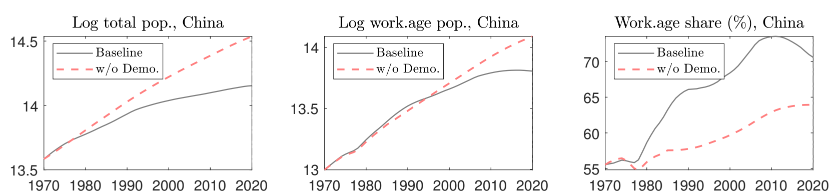

Figure F.1
Demographic process

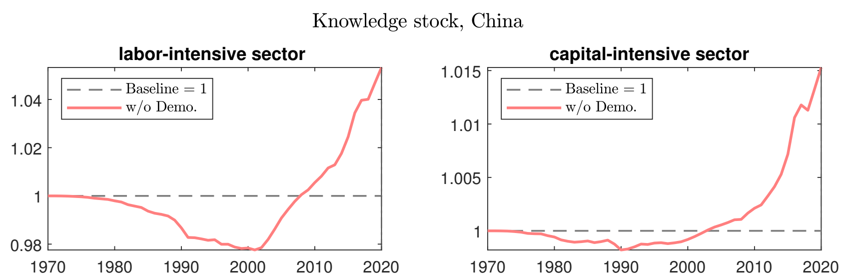

Figure F.2
Knowledge stocks

F.2. Model based projection

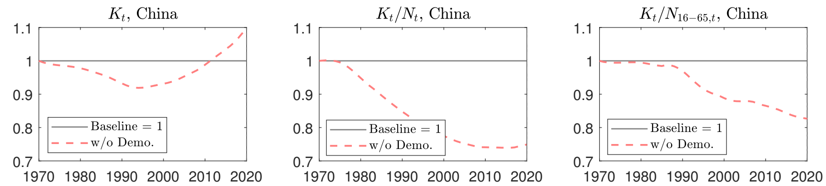

FIGURE F.3
CAPITAL STOCKS

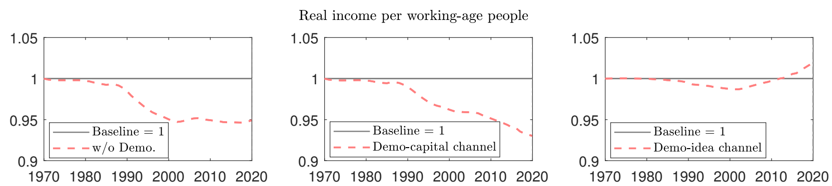

FIGURE F.4
REAL INCOME PER WORKING-AGE PEOPLE

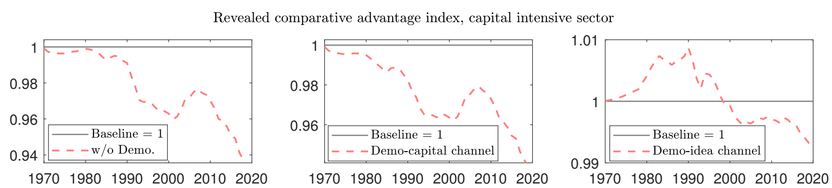

FIGURE F.5
REVEALED COMPARATIVE ADVANTAGE INDEX

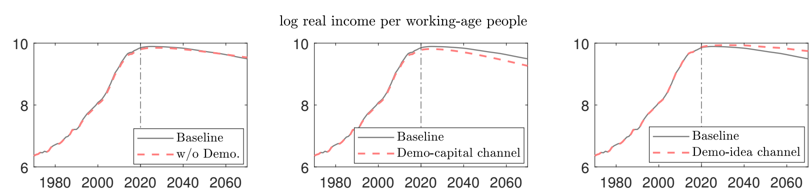

FIGURE F.6
REAL INCOME PER WORKING-AGE PEOPLE

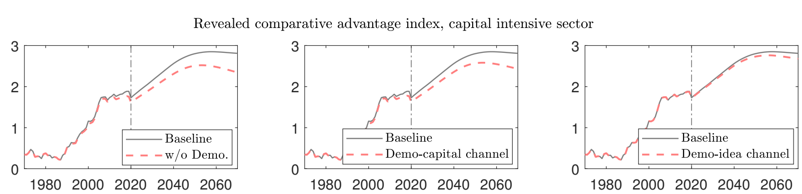

FIGURE F.7
REVEALED COMPARATIVE ADVANTAGE INDEX